

# UNCLASSIFIED

AD NUMBER
AD218572
NEW LIMITATION CHANGE
TO Approved for public release, distribution unlimited
FROM Distribution authorized to U.S. Gov't. agencies and their contractors; Administrative/Operational Use; MAY 1959. Other requests shall be referred to Office of Naval Research, One Liberty Center, Suite 1425, 875 North Randolph Street, Arlington, VA 22203-1995.
AUTHORITY
ONR ltr dtd 28 Jul 1977

THIS PAGE IS UNCLASSIFIED

**UNCLASSIFIED**

**A218572**

**Armed Services Technical Information Agency**

**ARLINGTON HALL STATION  
ARLINGTON 12 VIRGINIA**

**FOR  
MICRO-CARD  
CONTROL ONLY**

**1 OF 2**

**NOTICE: WHEN GOVERNMENT OR OTHER DRAWINGS, SPECIFICATIONS OR OTHER DATA ARE USED FOR ANY PURPOSE OTHER THAN IN CONNECTION WITH A DEFENSE RELATED GOVERNMENT PROCUREMENT OPERATION, THE U. S. GOVERNMENT THEREBY INCURS NO RESPONSIBILITY, FOR ANY OBLIGATION WHATSOEVER; AND THE FACT THAT THE GOVERNMENT MAY HAVE FORMULATED, FURNISHED, OR IN ANY WAY SUPPLIED THE SAID DRAWINGS, SPECIFICATIONS, OR OTHER DATA IS NOT TO BE REGARDED BY IMPLICATION OR OTHERWISE AS IN ANY MANNER, LICENSING THE HOLDER OR ANY OTHER PERSON OR CORPORATION, OR CONVEYING ANY RIGHTS OR PERMISSION TO MANUFACTURE, USE OR SELL ANY PATENTED INVENTION THAT MAY IN ANY WAY BE RELATED THERETO.**

**UNCLASSIFIED**

An Investigation of  
THE FRACTURE OF METALS

Technical Report No. 2

THE EFFECT OF SECOND PHASES  
ON  
THE MECHANICAL PROPERTIES OF ALLOYS

By

B. I. Edelson  
W. M. Baldwin, Jr

Conducted by

DEPARTMENT OF METALLURGICAL ENGINEERING  
CASE INSTITUTE OF TECHNOLOGY

In Cooperation With

OFFICE OF NAVAL RESEARCH, U. S. Navy

Contract No Nonr-1141(04)

Authority NR 031-049/9-19-56

Cleveland, Ohio

May 1959

Reproduction in whole or in part is permitted for any purpose of the  
U S Government

DEPARTMENT OF METALLURGICAL ENGINEERING  
CASE INSTITUTE OF TECHNOLOGY

Technical Report No. 2

THE EFFECT OF SECOND PHASES  
ON  
THE MECHANICAL PROPERTIES OF ALLOYS

Written By.

Burton I. Edelson  
B. I. Edelson

W. M. Baldwin, Jr.  
W. M. Baldwin, Jr.

Approved By:

W. M. Baldwin, Jr.  
W. M. Baldwin, Jr.  
Task Order Director

Distribution List For  
Technical Report  
No. 2

Contract Nonr-1141(04)

May, 1959

Copy No. \_\_\_\_\_

NAVY

- |     |  |       |  |
|-----|--|-------|--|
| 1-2 | Chief of Naval Research<br>Department of the Navy<br>Washington 25, D. C.<br>Attn: Code 423  | 9-17  | The Director, Naval Res. Lab.<br>Washington 25, D. C.<br>Attn: Technical Information<br>Officer  |
| 3   | Commanding Officer<br>Office of Naval Research<br>Branch Office<br>495 Summer Street<br>Boston 10, Massachusetts                                       | 18    | Director<br>David Taylor Model Basin<br>Washington 7, D. C.  |
| 4   | Commanding Officer<br>Office of Naval Research<br>Branch Office<br>John Crerar Library Bldg.<br>10th Floor, 86 E. Randolph St.<br>Chicago 11, Illinois | 19-20 | Director, Naval Res. Laboratory<br>Washington 25, D. C.<br>Attn: Code 2500, Metallurgy<br>Code 2020, Tech. Library                         |
| 5   | Commanding Officer<br>Office of Naval Research<br>Branch Office<br>801 Donahue Street<br>San Francisco 24, Calif                                       | 21-24 | Bureau of Aeronautics<br>Department of the Navy<br>Washington 25, D. C.<br>Attn: N. E. Promisel, AE-41(3)<br>Tech. Library, TD-41(1)       |
| 6   | Commanding Officer<br>Office of Naval Research<br>Branch Office<br>1030 Green Street<br>Pasadena, California   | 25    | Commanding Officer<br>Naval Air Material Center<br>Naval Base Station<br>Philadelphia, Penna<br>Attn: Aeronautical Materials<br>Laboratory |
| 7   | Commanding Officer<br>Office of Naval Research<br>branch Office<br>Navy #100, Box 39<br>Fleet Post Office<br>New York, N. Y.                           | 26-29 | Bureau of Ordnance<br>Department of the Navy<br>Washington 25, D. C.<br>Attn: Rex (3)<br>Technical Library AD3(1)                          |
| 8   | Contract Administrator<br>SE Area, Office of Naval Res<br>Department of the Navy<br>Washington 25, D. C.<br>Attn Mr R F Lynch                          | 30    | Superintendent, Naval Gun Factory<br>Washington 20, D. C.<br>Attn: Metallurgical Lab. IN910  |
|     |  | 31    | Commanding Officer<br>U. S. Naval Ordnance Laboratory<br>White Oaks, Maryland  |

32 Commanding Officer  
U. S. Naval Ordnance Test Station  
Inyokern, California

33-37 Bureau of Ships  
Department of the Navy  
Washington 25, D. C.  
Attn: Code 343 (3)  
Code 337L, Tech. Lib. (1)  
Code 692 (1)

38 U. S. Naval Engineering Experiment Station  
Annapolis, Maryland  
Attn: Metals Laboratory

39 Director, Materials Laboratory  
Building 291  
New York Naval Shipyard  
Brooklyn 1, New York  
Attn: Code 907

40 Bureau of Yards and Docks  
Department of the Navy  
Washington 25, D. C.  
Attn: Research and Standards Div.

41 Commanding Officer  
Naval Proving Grounds  
Dahlgren, Virginia  
Attn: Laboratory Division

#### ARMY

42 Chief of Staff, U. S. Army  
The Pentagon  
Washington 25, D. C.  
Attn: Director of Research and Development

43-45 Office of Chief of Ordnance  
Research and Development Service  
Department of the Army  
Washington 25, D. C.  
Attn: ORDTB

46 Commanding Officer  
Watertown Arsenal  
Watertown, Massachusetts  
Attn: Laboratory

47 Office of Chief of Engineers  
Department of the Army  
Washington 25, D. C.  
Attn: Research and Development Branch

#### AIR FORCES

48 U. S. Air Forces  
Research and Development Div.  
The Pentagon  
Washington 25, D. C.

49-50 Air Materiel Command  
Wright-Patterson Air Force Base  
Dayton, Ohio  
Attn: Materials Laboratory  
MCREXM

#### OTHER GOVERNMENT AGENCIES

51 Atomic Energy Commission  
Division of Research  
Metallurgical Branch  
Washington 25, D. C.

52 National Bureau of Standards  
Washington 25, D. C.  
Attn: Physical Metallurgy Division  
Technical Library

53 National Advisory Committee  
for Aeronautics  
1724 F Street, N. W.  
Washington 25, D. C.

54 Research and Development Board  
Committee on Basic Physical  
Sciences  
The Pentagon  
Washington 25, D. C.  
Attn: Metallurgy Panel

55 U. S. Atomic Energy Commission  
Library Branch, Tech. Inf  
Service, ORE  
P. O. Box E  
Oak Ridge, Tennessee

56 Los Alamos Scientific Lab.  
P. O. Box 1663  
Los Alamos, New Mexico  
Attn: Document Custodian

57 U. S. Atomic Energy Commission  
New York Operations Office  
P. O. Box 30, Ansonia Station  
New York, 23, N. Y.  
Attn: Division of Tech. Inf. and  
Declassification Service

58 Oak Ridge National Laboratory  
P. O. Box P  
Oak Ridge, Tennessee  
Attn: Central Files

OTHERS

59 Dr. E. P. Klier  
Department of Metallurgy  
University of Maryland  
College Park, Md.

60 Dr. D. S. Clark  
Department of Mech. Engr.  
California Institute of Tech  
Pasadena, California

61-62 University of Illinois  
Urbana, Illinois  
Attn: Dr. N. M. Newmark  
Dr. T. J. Dolan

63 Department of Metallurgy  
University of Pennsylvania  
Philadelphia, Penna

64 Professor M. Cohen  
Department of Metallurgy  
Massachusetts Inst. of Tech  
Cambridge 39, Mass

65 General Electric Company  
Research Laboratories  
Schenectady, New York  
Attn: J. H. Hollomon

66 Dr. R. F. Mehl  
Director of Metals Research Lab.  
Carnegie Institute of Tech.  
Pittsburgh, Penna

67 Brookhaven National Laboratory  
Information and Publication Div.  
Documents Section  
Upton, New York  
Attn: Miss Mary E. Waisman

68 Carbide and Carbon Chemicals Div.  
Plant Records Department  
Central Files (K-25)  
P. O. Box P  
Oak Ridge, Tennessee

69 Carbide and Carbon Chemicals Div.  
Central Reports and Information  
Office  
P. O. Box P (Y-12)  
Oak Ridge, Tennessee

70 General Electric Company  
Technical Services Division  
Technical Information Group  
P. O. Box 100  
Richland, Washington  
Attn: Miss M. G. Freidank

71 Dr. M. Gensamer  
Columbia University  
New York, N. Y.

72 Iowa State College  
P. O. Box 14A, Station A  
Ames, Iowa  
Attn: Dr. F. H. Spedding

73 Knolls Atomic Power Laboratory  
P. O. Box 1072  
Schenectady, New York  
Attn: Document Librarian

- |       |  |       |  |
|-------|--|-------|--|
| 74    | Dr. G. A. Nothmann, Manager<br>Applied Mechanics Division<br>Armour Research Foundation<br>Chicago, Illinois   | 84    | Westinghouse Electric Corp.<br>Atomic Power Division<br>P. O. Box 1468<br>Pittsburgh 30, Penna.<br>Attn: Librarian |
| 75    | Dr. W. C. MacGregor<br>Dept. of Mech. Engr.<br>Massachusetts Inst of Tech.<br>Cambridge, Massachusetts   | 85-89 | Armed Services Technical<br>Information Center<br>Documents Service Center<br>Knott Building<br>Dayton 2, Ohio     |
| 76    | Armour Research Foundation<br>Metals Research Division<br>35 W. 33rd Street<br>Chicago, Illinois<br>Attn. Librarian                                    | 90    | Dr. W. M. Baldwin, Jr.<br>Case Institute of Technology   |
| 77    | Sandia Corporation<br>Sandia Base<br>Classified Document Division<br>Albuquerque, New Mexico<br>Attn: Mr. Dale N. Evans                                | 91    | Dean Elmer Hutchisson<br>Case Institute of Technology  |
| 78    | Dr. C. S. Smith<br>Institute for the Study of Metal<br>University of Chicago<br>Chicago, Illinois  | 92    | Dr. A. R. Troiano<br>Case Institute of Technology  |
| 79-80 | University of California<br>Engineering Department<br>Berkeley, California<br>Attn: Dr. J. E. Dorn<br>Dr. E. R. Parker                                 | 93    | Dr. L. J. Ebert<br>Case Institute of Technology  |
| 81    | Professor F. A. Biberstein<br>Department of Mech. Engr.<br>Catholic University of America<br>Washington, D. C.   | 94-95 | Department of Metallurgical<br>Engineering<br>Case Institute of Technology<br>(File Copy)<br>Librarian             |
| 82    | Professor W. Prager<br>School of Applied Mathematics<br>Brown University<br>Providence, Rhode Island   |       |  |
| 83    | University of California<br>Radiation Laboratory<br>Information Division<br>Room 128, Building 50<br>Berkeley, California<br>Attn: Dr. R. K. Wakerling |       |  |



**THE EFFECT OF SECOND PHASES  
ON  
THE MECHANICAL PROPERTIES OF ALLOYS\***

by

**B. I. Edelson\*\* and W. M. Baldwin, Jr. \*\*\***

**ABSTRACT**

Tensile test data were determined for two-phase copper-base alloys fabricated synthetically by powder metallurgical methods with various second phase particles including metals, non-metals, and voids with a twenty-fold range in particle size in some series and with volume fractions ranging as high as 0.24. Only those second phase particles which developed a strong particle-matrix bond strengthened the alloys and in those cases yield stress  $\sigma$  depended upon mean free path  $\lambda$  between particles. The Gensamer relationship,  $\sigma = -A \log \lambda + B$ , was followed only within certain limits of mean free path. All second phase


.....  
\* This paper is based upon a portion of a research program conducted in the Department of Metallurgical Engineering, Case Institute of Technology, in cooperation with the Office of Naval Research. The data were used as the basis of a thesis submitted by Lt. Cmdr. Edelson to Yale University in partial fulfillment for the Degree of Doctor of Philosophy.

\*\* Lieutenant Commander U S Navy: Bureau of Ships, Navy Department, Washington, D C

\*\*\* Research Professor, Case Institute of Technology, Cleveland, Ohio

particles as well as voids were found to embrittle the alloys in a manner which depended upon volume fraction of second phase only and which was independent of particle size, shape, and composition.

It was hypothesized that second phases are embrittling because they serve to concentrate strain (not stress) along slip lines (in the sense of the theory of plasticity) wherein the metal reaches its fracture strain at a low external average strain. This rationalization finds support in the fact that the curves for ductility vs the volume fraction of second phase are quite similar to the curves for ductility vs. the fractional area removed in notch tensile tests. Strain hardening exponent and fracture stress behaved in a similar fashion to ductility.



## INTRODUCTION

This is a report of an experimental investigation into the effects of a second phase -- its volume fraction, particle size, shape, interfacial bond, and chemical composition -- on some mechanical properties -- yield stress, strain hardening exponent, ductility, fracture stress and engineering tensile strength -- of a two-phase alloy.

Two phases can coexist in the same three-dimensional space as two discontinuous phases (a rare situation), two interpenetrating continuous phases, or one discontinuous phase embedded in a continuous phase. Fig. 1 shows examples of all three possibilities. The present report concerns itself with the last of these three situations exclusively.

The volume fraction,  $f$ , and particle size,  $d$ , of a discontinuous phase embedded in a continuous phase are independent variables. They may be combined into such functions as mean free path,  $\lambda = \frac{2d}{3f}(1 - f)$ , or interparticle spacing  $D_s = d(1 - f)\sqrt{\frac{2}{3f}}$ . Fig. 2 gives a graphical interpretation of these derived functions.

Do mechanical properties depend upon volume fraction alone? Does particle size have some effect? If so, is the effect such that it is mean free path or interparticle spacing that is the true variable in question? The technical literature offers no answer as far as the strain hardening exponent, ductility, or fracture stress is concerned and as for yield stress it is unsettled in two respects. There is contention as to the con-

trolling variable for yield stress. For example, Gensamer's commonly quoted work (1), (2) has it that yield stress is a function of mean free path,  $\lambda$ ; Roberts, Carruthers and Averbach (3), Shaw, Shepard, Starr, and Dorn (4) and Turkalo and Low (5) agree with Gensamer; Gregory and Grant (6) and Lenel, Backensto, and Rose (7) feel that yield stress depends upon interparticle spacing; while Keeler (8) (9) denies this and feels it is a function of volume fraction,  $f$ , alone, particle size,  $d$ , being without effect on the property. Secondly, there is contention as to what particular function of a given variable yield stress follows. For example, yield stress,  $\sigma$ , is reported to be related to mean free path,  $\lambda$ , according to the following functional relations (in which all the A's and B's are different constants)

$$\sigma = -A \log \lambda + B$$

$$\sigma = -A \lambda^n \quad (0.28 < n < 0.15)$$

$$\sigma = A e^{-B\lambda} + C$$

by Gensamer (1) (2), Dorn (4), and Unckel (10) respectively.

We are considering here and throughout the rest of the report only second phases which differ significantly in hardness from the matrix (being harder or softer). Hehemann, Luhan, and Troiano (11) have already demonstrated that a second phase has less and less effect on the properties of an alloy as its hardness approaches that of the surrounding continuous phase.

To critically identify the true factors on which yield strength (or any other mechanical property) depends, both volume fraction,  $f$ , and particle diameter,  $d$ , must be independently varied in tensile tests. The need for this is readily appreciated by referring to Fig. 3. Here a given property,  $P$ , is plotted against the two factors, volume fraction,  $f$ , and reciprocal mean free path,  $1/\lambda$ . Let us assume for the moment that the property,  $P$ , really depends upon volume fraction,  $f$ . In this case, the function describing the property is a cylindrical sheet parallel to the  $1/\lambda$  - axis. A single run of experiments in which both  $f$  and  $\lambda$  might be varied (but not independently) along some curve such as i in Fig. 3a would yield property values given by the curve ii. The projection of this curve on the  $P$ - $f$  plane gives curve iii (in this case the functional relation) while the projection on the  $P$  -  $1/\lambda$  plane gives iv. Without further knowledge, the experimenter does not know which projection is the correct one, and if prejudiced, may choose one without even considering the other. He is open to a double error if he chooses incorrectly for any functional relation between the property and reciprocal mean free path in the present illustration (such as  $P = A \log \lambda$ , etc.) will depend upon the course of the original curve i. If, on the other hand, tensile tests are performed on specimens in which  $f$  and  $1/\lambda$  are independently varied -- say  $1/\lambda$  being varied while  $f$  is held constant at a number of values, as illustrated in Fig. 3b by curves i, ii, and iii -- then the

projections of the corresponding property curves iv, v, and vi on the  $P - f$  plane form a common curve, vii (the true functional relation), while they give three separate projections on the false  $P - 1/\lambda$  plane. In this case a critical identification of the true factor influencing the property in question becomes possible.

With this in view the present investigation incorporated a test program in which the volume fraction,  $f$ , and the particle diameter,  $d$ , of the second phase were independently varied. The mechanical properties - yield stress, strain hardening exponent, ductility, engineering tensile strength and fracture stress - were plotted against the volume fraction of second phase particles, the mean free path between particles, and the mean interparticle distance. That variable for which the data gave a single curve was adjudged the true factor, those for which the data gave separate curves were rejected as false. A separate evaluation had to be made for each property for it turns out that different properties are differently controlled. The quantities  $f$  and  $d$  were varied over the widest range possible within experimental feasibility to insure a split of the curves when falsely plotted, especially in the event where the property changes slowly with a change in its governing factor.

In order to deliberately control the volume fraction and particle size of the second phase it was decided to prepare two-phase alloys by powder metallurgical methods. A practical difficulty arises in this con-

nection about which some detailed comment ought to be made. Ordinarily, pressing and sintering metal powders yields a compact that is short of theoretical density by several percent. This shortage in density is due to holes or voids which in themselves must be counted as a second phase having significantly different hardness from the matrix. Cold-working and annealing pressed and sintered compacts virtually eliminates these voids, but the addition of second phases, as will be shown, reduces ductility and thus prevents the full use of cold-working for this purpose. (As a matter of fact, the standard amount of cold-working finally adopted -- that which could be carried out under the wide range of volume fractions of the second phase deemed necessary for the main purpose of this investigation still left 2 percent voids in the matrix). We are thus faced with questions involving the additive effects of holes and second phases on mechanical properties. To resolve these questions two-phase alloys were prepared in matrices of constant hole content and size (2 percent and 0.00005 inches average diameter) and results are plotted on linear scales using total volume fraction (the volume fraction of both holes and second phase) or total reciprocal mean free path (the reciprocal mean free path of both holes and second phase, etc.). The advantages of this procedure will become evident in the discussion of the results.

The details of procedure - the methods of preparing the tensile specimens, the several microstructures obtained, the methods of determining volume fraction, particle size and their related quantities, and the methods of tensile testing -- are given in Appendix I.



## RESULTS

It was noted that tensile specimens produced from powders possess voids. Copper specimens containing various quantities of holes were produced in three ways: (a) by varying the amount of swaging, (from 13 to 70% reduction in area) after the complete compacting and sintering process, (b) by varying the compacting pressure (from about 30,000 to 50,000 psi), and (c) by incorporating various amounts of subliming powder (up to 10 volume percent  $\text{NH}_4\text{HCO}_3$ ) in the original compact. (Details were given previously). All of these treatments, while they gave a wide variety of volume fractions of voids (up to 10 percent), did not yield holes of varying diameter (these remained about 0.00005 inches in diameter). The data shown in Fig. 4, therefore, are not intended to demonstrate that the tensile properties shown there are functions of volume fraction alone (although it will turn out that some of them are). It will be noted, however, that yield stress and engineering tensile strength are relatively unaffected by holes, whereas ductility and fracture stress (which depends on ductility) are strongly affected. The standard pressing, sintering, swaging and annealing schedule adopted for preparing the two-phase alloys whose properties are about to be described yielded about 2 percent voids

### Yield Stress

The yield stresses of two-phase alloys are plotted in Fig. 5 The

data for graphite, lead, and molybdenum are not critical since they are for one particle size only. It is to be noted, however, that within the experimental range they display no hardening. The data for alumina, iron, and chromium are critical since both size and quantity are varied. Of these, alumina shows no hardening, but the other two do. Of these latter two, both indicate that yield stress depends upon both volume fraction and particle size and, in fact, on mean free path. It is noteworthy that hardening falls off above a critical reciprocal mean free path (below a critical mean free path) and that this reciprocal value is lower the smaller the particle size. It is to be remembered that the abscissae here are the totals of the volume fractions reciprocal mean free paths, etc., of both the second phases and the voids in the matrix, but that the holes in the matrix of the two phase alloys are of fixed quantity and size. The importance of this standardization can be appreciated from the results shown in Fig. 6a where varying quantities of iron (0.0013 inch diameter) and molybdenum (0.00019 inch diameter) were added to a copper matrix (still containing 2 percent voids). The yield stresses of these alloys when plotted against total reciprocal mean free path scatter between the curve for iron alone which showed hardening and molybdenum alone which showed no hardening. When the data are plotted as in Fig. 6b against the reciprocal mean free path of iron plus holes only the points fall nicely along the curve for iron obtained in Fig. 5.

### Ductility

Fig. 7 presents the ductility of the alloys studied in this investigation as a function of volume fraction of the second phase, the reciprocal of the mean free path, and the reciprocal of the mean particle spacing. It includes, also, similar plots constructed from data reported by Zwilsky and Grant (12) for Cu - Al<sub>2</sub>O<sub>3</sub> compacts and from data kindly furnished by Miss Turkalo gathered for (though not reported in) the Turkalo and Low paper (5) for quenched and tempered steels having various quantities and sizes of tempered carbides as a second dispersed phase. \* The evidence is clear: ductility, unlike yield stress, is a function of volume fraction,  $f$ , and is unaffected by particle size,  $d$ . It is to be noted that all second phases, whether they served to increase yield stress or not, were embrittling. For example, alumina did not increase yield stress for any of the sizes and quantities studied (Fig. 5j), but did embrittle (Fig. 7j); on the other hand, both the finer sizes of chromium particles (Fig. 5d) and Turkalo and Low's carbide particles in steel which upped yield stress were embrittling (Figs. 7d and p).

Fig. 8 contains ductility data for various alloys plotted together

- - - - -  
\* Turkalo and Low reported two sets of volume fractions for their alloys, that computed from a lineal analysis of electron micrographs and that computed from chemical analysis. We have used the former of the two sets on the advice of Miss Turkalo.

all against total volume fraction (again, particles plus voids). Attention is drawn especially to the points for the series of alloys simultaneously containing fine molybdenum and coarse iron powders (0.00019 and 0.0013 inches diameter respectively). A single coherent curve results when the ductility of these alloys is plotted against the volume fraction of holes plus iron plus molybdenum, whereas it will be recalled iron and molybdenum had totally different effects on yield stress.

Even more startling is the fact that the ductility vs. volume fraction curve is the same for the copper matrix alloys irrespective of the nature of the second phase-holes, chromium, alumina, etc. -- as Fig. 8 shows. Also included in Fig. 8 are not only Zwilsky and Grant's data for  $\text{Cu} - \text{Al}_2\text{O}_3$ , but also some data they report for  $\text{Cu} - \text{SiO}_2$  compacts. These were for one particle size only and hence could not be used in Fig. 7 to critically test what factor ductility depends upon. On the other hand, if it is now granted that ductility is a function of volume fraction only, then the data are of use in comparing the effects of different second phases on the ductility vs. volume fraction curve.

### Strain Hardening Exponent

The stress-strain diagrams of the alloys studied in this investigation could not be characterized by a single strain hardening exponent throughout their entire course -- indeed this is true of all stress-strain

diagrams. Fig. 9 gives a group of stress-strain diagrams for the series of copper alloys containing various quantities of 0.0016 inch diameter chromium particles and it is seen that the curves are not single straight lines. The exponents reported here are the slopes of the latter parts of the (log stress-log strain) curves and can only be taken as a rough description of this overall strain hardening behavior of the alloys investigated here. Fig. 10 shows the strain hardening exponent plotted against volume fraction and reciprocal mean free path. Like ductility, the strain hardening exponent appears to be a function of the volume fraction and not of mean free path. \* Fig. 11 assembles the exponent vs. volume fraction curves for all the second phases. They do not fall so clearly on a single curve as did the ductility data.

#### Fracture Stress

The fracture stresses of the various alloys are plotted against volume fraction of particles and reciprocal mean free path between particles in Fig. 12. The data in general favor a volume fraction relation. When fracture stress vs. volume fraction curves for the different second phases are assembled a rough trend curve is obtained as shown in Fig. 13.

-----  
\* A plot of the data vs. reciprocal mean particle spacing shows even greater dispersion than that found when reciprocal mean free path is used.

## DISCUSSION

The results indicate that of the alloys investigated chromium and iron as second phases served to increase yield stress; molybdenum, alumina, graphite, lead and voids did not. Where yield stress was increased it was a function of the mean free path between second phase particles and not a function of volume fraction alone (or mean particle spacing). All of the second phases were embrittling and ductility was a function of the volume fraction of the second phase and not a function of mean free path between particles. This function was independent of the nature of the second phase whether that was voids, chromium, iron, alumina, molybdenum or silica. The strain hardening exponent and fracture stress in general behaved like ductility.

The largest problem here is to explain why hardening is a function of mean free path but embrittlement is a function of volume fraction. One might properly ask whether this behavior is general or just specific to the specimens produced by the powder metallurgical technique used here, assuming (as has been suggested several times in powder metallurgy symposia, see (13) for example) that the bonding is so weak as to break down after even slight deformation so that effectively all the second phases soon become holes. Yet Turkalo and Low's steel specimens (see (5) and Fig. 7) in which the second phases were produced by

more natural techniques behaved as did the specimens produced by powder metallurgical methods. Furthermore, micrographs of regions close to the fracture surface (where deformation is high) show the second phases to be firmly embedded in the matrix with no evidence of voids between the second phase and the matrix in the direction of tension which would be the case if the bonding had broken down (see Fig. 14). Many particles, in fact, were found to be clinging to the very surface of fracture by considerably less than 50 percent of their surface area. We are forced to give serious consideration, then, to the fact that the dependence of ductility upon volume fraction is a fundamental law governing the deformation behavior of all two-phase alloys and not merely a demonstration of the peculiar properties of a hothouse variety of synthetic aggregates.

One might attempt to explain the embrittling effect of second phases on an alloy on the basis that the second phase is inert and does not join in the deformation, so that ductility of the aggregate is reduced in direct proportion to the participating matrix. While this explanation is compatible with the observation that ductility depends upon the volume fraction of the second phase alone and not upon its particle size, and that the embrittlement is independent of the nature of the second phase (provided it is substantially harder than the matrix), its requirement of a linear decrease in ductility (computed now as conventional

percent reduction in area) with increase in volume fraction of the second phase would fall wide of the observed ductility -- volume fraction curve.

Instead, we shall call upon the fact that a notch or a discontinuity in an otherwise uniform plastic mass is a strain concentrator. (Notice the emphasis on strain concentration here, not upon stress concentration.) For example, for an ideal rigid plastic mass, the mathematical theory of plasticity predicts strain to be concentrated along definite lines when a notched bar is pulled in plane strain (14). Real metals will not behave so ideally: strain will spread out from the ideal predicted lines, but the strain is still heavily concentrated as shown in Fig. 15. One anticipates that those metals with low strain hardening will approach ideal behavior, while those with high strain hardening will show less strain concentration for a given notch geometry. It is suggested here that the role of a uniformly randomly dispersed second phase is to concentrate strain within or near some skeletal pattern, and that this concentration of strain causes the metal to reach its fracture strain locally within the skeletal pattern at a much lower external average strain. Geometric similitude would dictate that, if the entire skeletal pattern corresponding to a given dispersion of a second phase, such as is shown in Fig. 15, were to be photographically enlarged, the strain pattern would merely be enlarged proportionately. The strain concentration



pattern would remain the same. So would the volume fraction of the second phase, even though the hole size per se would be greater. We thus come to an understanding of why embrittlement by a second phase is independent of particle size and depends only on the volume fraction. This reasoning finds support in the fact that the ductility vs. volume fraction curve for the two-phase alloys is about the same as the ductility vs. notch depth curve for copper as shown in Fig. 16.

On the other hand, it is anticipated that the closer one brings holes of a given size toward each other the greater will be the concentration of strain and the consequent embrittlement. This would account for the increased embrittlement as the volume fraction of a second phase is increased

It must be acknowledged that the details of the configuration of the regions in which strain will be concentrated by a uniformly random distribution of a very soft dispersed phase (e. g. holes) or a very hard dispersed phase (e. g. chromium in copper) will be different, but in the main, the skeletal patterns must be quite similar and this is reflected in the fact that the ductility vs. volume fraction curves for all copper alloys studied was the same as Fig. 8 showed.

While all of the second phase particles as well as voids embrittled the alloys, only two second phases -- iron and chromium -- imparted any significant strengthening effect. The most obvious differ-

ence between the particles which did strengthen and those which did not is their probability of bonding firmly with the copper matrix. It is recognized that the possibility of different degrees -- even different kinds -- of bonding exists in the systems studied in this investigation. Iron and chromium have reasonable solubilities in copper (4.5 and 1.5 percent, respectively) at the sintering and annealing temperatures used in preparing the specimens, and fairly strong bonds may have been attained. Molybdenum, on the other hand, has a vanishingly small solubility in copper (15), while alumina and graphite being non-metallic structures could at best have developed bonds no stronger than van der Waals forces.

The dependence of strengthening upon the existence of strong particle-matrix bonding is well covered in the literature. Unckel (10) predicated his mechanism of internal stressing due to particles upon the presence of such bonds capable of supporting shear stress across the interfaces. Gurland and Norton, too, in their treatment of the role of the binder phase cobalt-tungsten carbide aggregates (16) concurred in this bonding requirement. The present results, then, support this previous work.

In the two systems where strengthening occurred -- copper-chromium and copper-iron -- the yield stress was shown by Fig. 5 to depend upon the mean free path between particles and holes. In order

to compare these results with quantitative predictions existing in the literature these yield stress data have been replotted in Fig. 17. This is a plot similar to that of Gensamer with yield stress plotted this time as a function of the logarithm of the reciprocal mean free path. In this particular plot, unlike all others in this report, the 2 percent of holes inherent in the matrix has been neglected and only the paths between second phase metal particles have been considered.

Fig. 17 shows that a linear region exists between certain limits of  $\log 1/\lambda$  only. There are three important features to be noted from this plot: (1) that above a critical mean free path (below a critical  $1/\lambda$ ) no strengthening occurs, (2) that within a middle region iron and chromium particles strengthen equally and in a linear fashion within the scatter of data, and (3) that for each size of particle a maximum of strengthening occurs after which a further decrease of mean free path (increase of  $1/\lambda$ ) the yield stress falls off. The linear region agrees with the prediction of Gensamer (1) (2) and of others (3) (5).

Although the data tend to support the Gensamer plot, in the linear region, the test cannot be considered critical. The data plotted on log-log paper after the method of Dorn et al (4) looks much the same.

The behavior of the strain hardening exponent was similar to that of ductility in that it followed the course of volume fraction alone. The ability of the matrix to strain harden has been described above as pre-

cisely that factor which determines the degree of strain concentration in the matrix which the second phase imposes. It would then necessarily follow that the two properties would show similar plots, that is, depend upon the same parameter -- in this instance volume fraction.

Lastly, the fracture stress also was found to depend upon volume fraction. In computation, the fracture stress (load at fracture divided by area of fracture) depends strongly upon the fracture area. The fact that the load at fracture did increase with yield stress may well explain the wider scatter of the fracture stress data. However, to the fact that fracture area was considerably the more widely varying quantity is attributed the similarity of behavior in the two quantities -- ductility and fracture stress

## CONCLUSIONS

From the preceding discussion the following conclusions are reached:

1. Only certain second phases strengthen their alloys
2. In order for particle strengthening to occur, firm particle-matrix bonding is required.
3. When strengthening occurs, yield stress depends upon mean free path.
4. The Gensamer relationship (stress varies linearly with the logarithm of mean free path between particles) holds true for those alloys in which strengthening occurs only within a limited range. For each particle size a minimum mean free path for strengthening is reached after which yield stress decreases.
5. All second phase particles as well as voids embrittle their alloys.
6. Ductility depends upon volume fraction alone, and is independent of particle size, shape, or composition.
7. Volume fractions of several second phases in the same matrix are additive in determining ductility.
8. The ductility curve for notched specimens of various notch fractions is similar to the curve for specimens containing various volume fractions of second phase particles.
9. The strain hardening exponent and fracture stress understandably behave like ductility, in that they depend upon volume fraction alone.
10. The above conclusions are valid within the scope of the present work: for particles of about 0.0002 inches (5 microns) and larger and for small voids; for volume fractions of from 0 to 25%; for slightly irregular and spherical shapes; and for several different hardness levels.

### ACKNOWLEDGMENTS

The authors wish to thank Messrs. George Condzer and Richard Howe of the Staff of the Department of Metallurgical Engineering, Case Institute of Technology for many kind services.

Appendix I

EXPERIMENTAL PROCEDURE

To meet all of these requirements set forth in the preceding sections tensile specimens were prepared by powder metallurgical methods from the alloy systems and in the ranges of volume fraction and particle size given in Table 1

TABLE 1

System <sup>a</sup>	Volume Fraction Range	Particle Size Range
Cu-voids	.005 - .10	0.00005"
Cu-Cr	0 - .24	0.00035" - 0.0084"
Cu-Fe	0 - .18	0.0013" - 0.0070"
Cu-Mo	0 - .18	0.00019"
Cu-Al <sub>2</sub> O <sub>3</sub>	0 - .22	0.00022" - 0.0023"
Cu-Pb	0 - .06	0.0029"
Cu-Graphite	0 - .05	0.00023"

<sup>a</sup> Copper is the continuous phase in all the systems listed

A description of the copper powder and the second phase powders and particles employed in this investigation is contained in Table 2.

Specimen Preparation - The preparation of the copper-dispersion aggregates followed the steps outlined below.

- (1) The powders were weighed on a balance. The total weight of each specimen was 75 grams, except for the case of Al<sub>2</sub>O<sub>3</sub> and graphite where their low density necessitated a reduction in total weight of each specimen sufficient to keep the volume

TABLE 2

## Composition of Powders Used

<u>Powder</u>	<u>Mfr. - Type</u>	<u>Comp.</u>	<u>Size</u>
<b>Copper</b>	Metals Disintegra- ting Co. Grade MD - 165	Cu-99.0% (Min)	+ 150 mesh .4% + 200 mesh 21.4% + 325 mesh 27.8% - 325 mesh 50.4%
<b>Molybdenum</b>	General Electric Lot MO - 225	Mo-99.98% (Min) Fe-.01%	+ 10 $\mu$ 47.2% - 10 $\mu$ 52.8%
<b>Chromium</b>	Met. Dis. Co. MD 301 MD 9689 150M	Cr-99.95% (Min) " Cr-97.8%	- 325 mesh - 20 + 50 mesh - 150 mesh
<b>Alumina</b>	Alcoa T - 61 (-28) Alcoa T - 61 (-60) Alcoa low iron A - 2 (-325)	Al <sub>2</sub> O <sub>3</sub> - 99+% " "	- 28 mesh - 60 mesh - 325 mesh
<b>Graphite</b>	National Carbon Co.	Reactor Grade C-99.9%	- 325 mesh
<b>Iron (Powder)</b>	Harshaw	Fe-Technical Grade	- 200 mesh
<b>Iron (Balls)</b>	Cleveland Abrasive Co.	Standard GCI	SAE 70
<b>Lead</b>	Belmont - Dust	Pb099.5% (Min)	.004" dia.



of the green compact constant. Pure copper control specimens consisted of 75 grams of copper, except for several specimens in which various amounts of  $\text{NH}_4\text{HCO}_3$  were mixed with the copper powder. The ammonium bicarbonate sublimed during the subsequent heating and introduced porosity according to the method of Duwez and Martens. (17)

- (2) The powders were mixed by hand for various periods of time in a pyrex tumbler. The time employed ranged from 10 minutes up to 1/2 hour depending on the type of second phase. The necessary time was judged by the homogeneity of the final mixtures
- (3) The mixed powders were cold-pressed for five minutes at 51300 psi in a punch and split die assembly. The resulting compacts measured 1.50 x 0.65 x 0.65 inches.
- (4) The green compacts were reduced in a hydrogen atmosphere for 12 hours at 900°F (482°C). Preliminary work indicated that this treatment was as effective as cleaning the powders prior to pressing.
- (5) The furnace temperature was then raised and the compacts were sintered in hydrogen for 4 hours at 1650°F (899°C) and furnace cooled.
- (6) The sintered compacts were annealed for 10 minutes in a  $\text{BaCl}_2$  salt pot at 1950°F (1066°C).

- (7) Following this last anneal the compacts -- now 1.55 x 0.65 x 0.65 -- were turned to .600" round cylinders. Several were turned to less than .600 round to determine the effect of percent reduction in area in swaging on density and resulting properties.
- (8) Only one cylinder was brought just to the melting point and allowed to solidify in a .600" round graphite crucible as a control. (This provided the specimen with density of 99.5% theoretical)
- (9) All cylinders were placed in standard copper water tube (ASTM B251 - 55T, Type L) OD .875", wall thickness, .045", about 15" long, 6 or 7 cylinders to a tube. Copper foil was used to plug the tube ends. The tubes were then swaged in 3 passes to .050" OD. Intermediate anneals of each tube between passes were made at 1300°F (704°C) for 10 minutes. The final diameter of the swaged copper cylinders was .420 -- a reduction in area of 51% for all standard specimens. A final anneal of 1 hour at 1300°F was provided after the final swaging. Theoretical densities of about 98% were obtained.
- (10) The copper cylinders were removed from the tubes by machining away the tubes. Tensile specimens were then machined from the copper rods.

Fig. 18 shows the copper compacts in each stage of preparation. Dimensions of the standard tensile specimens are provided in Fig. 19. Notched tensile specimens were also machined from the unalloyed copper. These specimens had notch angles of 30 and 90° and notch depths up to 30%. Some typical microstructures may be seen in Figs. 20 and 21.

Tensile Tests - All specimens were tested in tension using a 10,000 pound Riehle tensile machine, and a specially designed concentric fixture, which produced less than 0.001" between specimen axis and loading axis. The rate of cross head travel was held constant at .05 inches/minute. Stress-strain curves were automatically recorded using an X - Y recorder the inputs to which were the actual load on the specimen read from a strain gage on a calibrated load member and the instantaneous specimen diameter read from a clip-on strain gage. Maximum load and fracture load were marked and converted to ultimate tensile strength and true fracture stress. Flow stress at .002, .01, .02, and .05 strains were extracted and computed from the stress-strain curves. True fracture ductility was computed from the formula:  $\epsilon = \ln A_0/A_f$ , where  $A_0$  and  $A_f$  are the original and fracture specimen cross section areas, which were measured on a Wilder micro projector. Density measurements were made by hydrostatic weighing.

### Determination of Particle Size, Mean Free Path, and Mean Particle Spacing

The volume fraction of the second phase (f) was determined from the known weight fraction (W) of the second phase for each specimen by:

$$f = \frac{WD_1}{(1-W)D_2 + WD_1}$$

where  $D_1$  is the density of the matrix (8.96 g/cm<sup>3</sup> for copper) and  $D_2$  the density of the second phase (handbook values used). Of course, for pure copper specimens where porosity alone was being determined for control purposes, f became the percent of holes and the actual density of each specimen (D) was used:

$$f = \frac{8.96 - D}{8.96}$$

Fullman's method (18) was used for measuring mean free paths and for determining particle sizes. The mean free path ( $\lambda$ ) was determined from his formula:

$$\lambda = \frac{1 - f}{N_1}$$

The number of particles transited by a random line per unit length ( $N_1$ ) was determined on polished specimens viewed under a microscope equipped with a filar eyepiece and a transiting stage with a vernier adjustment. Many transits (over 1000 particles) were made on individual specimens until a good reproducible average for  $N_1$  was obtained.

Having determined  $\lambda$ , it was a simple matter to determine the average spherical particle diameter (d) using the formula.

$$d = \frac{3 f \lambda}{2 (1 - f)}$$

A spherical particle shape was assumed. In the case of spherical particles,  $d$ , then, is the actual particle diameter. For irregular-shaped particles, however,  $d$  is the diameter of an equivalent spherical particle which would produce the same MFP.

Once the particle size was determined for a few specimens of one series and reasonable reproducibility established, this average particle diameter was used to determine  $\lambda$  for the rest of the series by the following relationship:

$$\lambda = \frac{2d}{3f} (1 - f)$$

As Fig. 2 has shown, the mean particle spacing on a plane,  $D_s$ , is a vastly different quantity from the mean free path,  $\lambda$ . Whereas the latter is the mean uninterrupted path between particles the former is the average distance between nearest neighbors on a plane. Particle spacing,  $D_s$ , may be approximated by  $1 - f$  times the diameter of a particle's circle of influence on a plane,  $D_i$ .

$$\frac{\pi D_i^2}{4} \cdot N_s = 1$$

Where  $N_s$  is the number of particles per unit area. Then if  $N_s$  is replaced by its value in terms of  $d$  and  $f$  and this equation is solved for  $D_s$  it may be shown that:

$$D_i = d \sqrt{\frac{2}{3f}} \quad \text{and} \quad D_s = d(1 - f) \sqrt{\frac{2}{3f}}$$

This formula was used in computing  $D_s$ . The quantity  $D_s$ , as well as  $\lambda$ , then, is a function of both  $f$  and  $d$ . But, whereas,  $\lambda$  varies roughly as

$1/f$  (considering  $1 - f$  nearly equal to 1),  $D_s$  varies as  $\sqrt{1/f}$ . Therefore, if both particle size and volume fraction are independently varied in a given test series, it is a simple matter to differentiate between a dependence upon  $\lambda$  or  $D_s$ , as the experimental results show.

In this investigation the reciprocals of both  $\lambda$  and  $D_s$  were employed in plotting for convenience in comparing the plots of properties against these quantities with plots against  $f$  alone.

## BIBLIOGRAPHY

1. M. Gensamer, E. B. Pearsall, W. S. Pellini, and J. R. Low, Jr., "The Tensile Properties of Pearlite, Bainite, and Spheroidite," Trans. ASM, 30, 983 (1942).
2. M. Gensamer, "Strength and Ductility", Trans. ASM, 36, 30 (1946)
3. C. S. Roberts, R. C. Carruthers and B. L. Averbach, "The Initiation of Plastic Strain in Plain Carbon Steels," Trans. ASM 44, 1150, (1952).
4. R. B. Shaw, L. A. Shepard, C. D. Starr, and J. E. Dorn, "The Effect of Dispersions on the Tensile Properties of Al-Cu Alloys," Trans. ASM, 45, 249 (1953)
5. A. M. Turkalo and J. R. Low, Jr., "The Effect of Carbide Dispersion on the Strength of Tempered Martensite," Trans. AIME, 212, 750 (1958).
6. E. Gregory and N. J. Grant, "High Temperature Strength of Wrought Aluminum Powder Products," J. Metals 6, 247 (1954), (Trans. AIME, 200).
7. F. V. Lenel, A. B. Backensto, and M. V. Rose, "Properties of Aluminum Powders and of Extrusions Produced from Them," J. Metals 9, 124 (1957), (Trans. AIME 209).
8. J. H. Keeler, "Tensile Properties of Zr-Cr Alloys - Particle Strengthening Effects," Trans. ASM, 48, 825 (1956).
9. J. H. Keeler, "Tensile Characteristics of Particle - Strengthened Alloys of Zr and Fe," J. Metals, 8, 486 (1956).
10. H. Unckel, "Zur Abhangigkeit der Mechanischen Eigenschaften von der Structur bei Zwei - Phasen - Legierungen", Metall, 5, 146 (1951).
11. R. F. Hehemann, V. J. Luhan and A. R. Troiano, "The Influence of Bainite on Mechanical Properties," Trans. ASM, 49, 409, (1957).

12. K. M. Zwilsky and N. J. Grant, "Copper - Silica and Copper - Alumina Alloys of High Temperature Interest," J. Metals 9, 1197, (1957), Trans. AIME, 209.
13. Discussion to Powder Metallurgy Symposium; J. Metals, 9, 357, (1957), Trans. AIME, 209.
14. W. Prager and P. G. Hodge, Jr., "Theory of Perfectly Elastic Plastic Solids," John Wiley and Sons, Inc., New York (1951).
15. M. Hansen, "Constitution of Binary Alloys," 2nd Edition, McGraw Hill, New York, 600 (1958)
16. J. Gurland and J. T. Norton, "Role of the Binder Phase in Cemented WC-Co Alloys, J. Metals 4, 1051 (1952), (Trans. AIME, 194).
17. P. Duwez and H. E. Martens, "The Powder Metallurgy of Porous Metals and Alloys," Trans AIME, 175, 848 (1948)
18. R. L. Fullman, "Measurement of Particle Sizes in Opaque Bodies," J. Metals, 5, 447 (1953); (Trans AIME, 197)

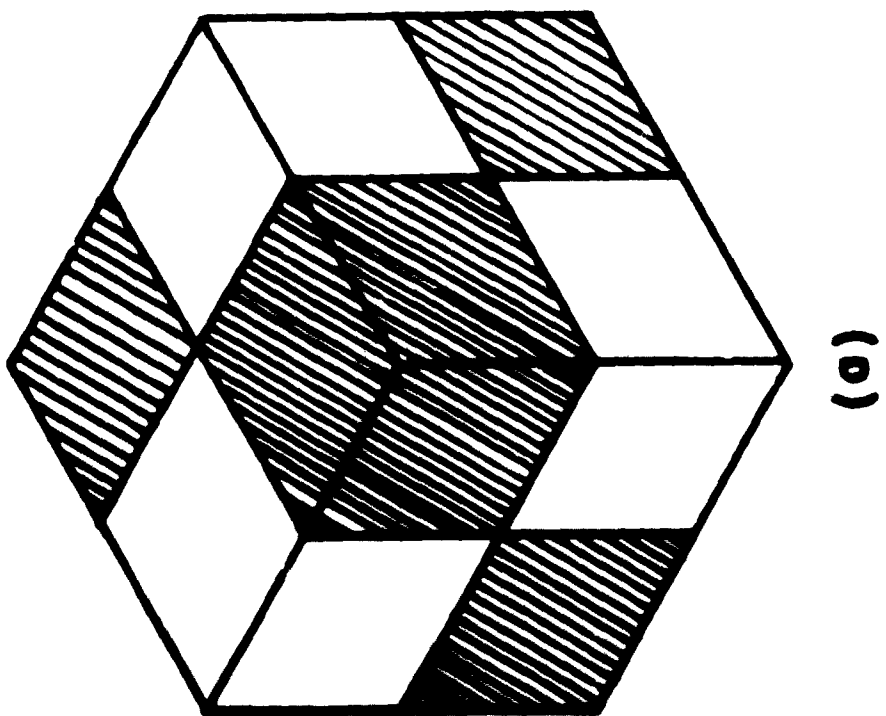


## LIST OF FIGURES

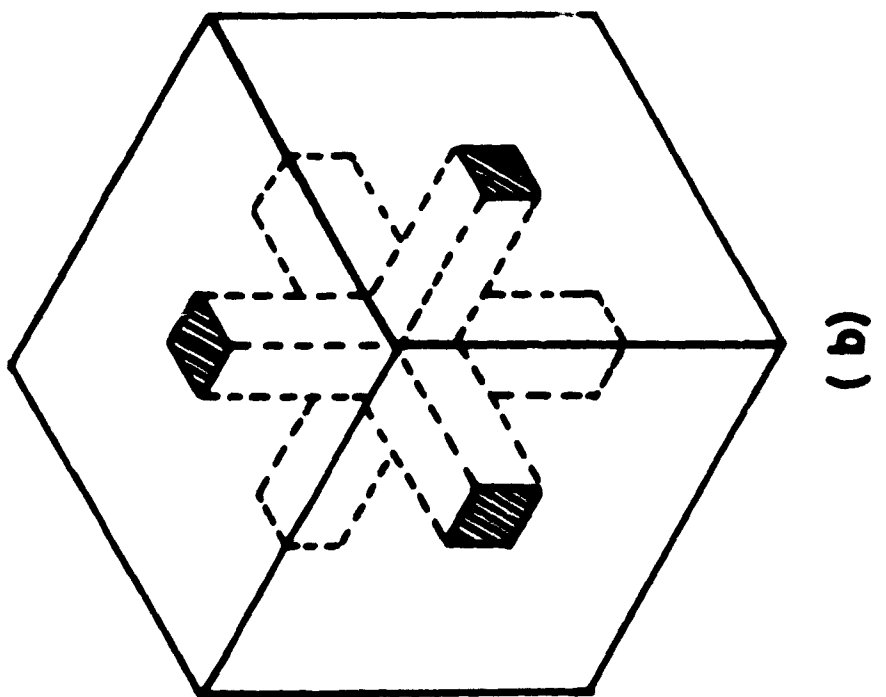
1. Three possible classes of two-phase alloys: two discontinuous phases, two continuous phases, and one continuous and one discontinuous phase. These blocks may be thought of as unit cells repeated ad infinitum in all three directions
2. Illustration of two measurements of particle spacing: mean free path between particles,  $\lambda$ , and interparticle spacing,  $D_g$ . Mean free path,  $\lambda$ , may be thought of as the distance one would move from a central reference particle (A in Fig. 2a) before impinging on a second particle taken as an average in all directions. Interparticle spacing may be thought of as the average diameter of space-filling cells centered on the dispersed particles
3. Generated surfaces for a mechanical property,  $P$ , which is a function of volume fraction,  $f$ , and which is independent of particle size,  $d$ , (and therefore mean free path,  $\lambda$ )
4. Several mechanical properties plotted against volume fraction of voids in pure copper compacts. Average void size: 0.00005" dia.
5. Yield stress at .002 strain for several copper dispersion alloys plotted against total volume fraction,  $f$ , (volume fraction of second phase plus volume fraction of voids in the matrix which, under the standard method of preparation, was two percent), total reciprocal mean free path,  $\lambda$ , (reciprocal mean free path of second phase plus reciprocal mean free path of voids in the matrix which under the standard method of preparation was 620 inches<sup>-1</sup>), and total reciprocal mean particle spacing,  $D_g$ , (reciprocal mean particle spacing of second phase plus reciprocal mean particle spacing of voids in the matrix which under the standard method of preparation was 3500 inches<sup>-1</sup>).
6. Yield stress of copper alloys containing particles of both iron and molybdenum and of iron alone plotted against reciprocal mean free path.
7. Ductility (natural strain at fracture --  $n A_o/A_f$ ) of several copper dispersion alloys plotted against three parameters of microstructure:

- (1) Volume fraction,  $f$
- (2) Reciprocal mean free path,  $1/\lambda$
- (3) Reciprocal mean particle spacing,  $1/D_s$

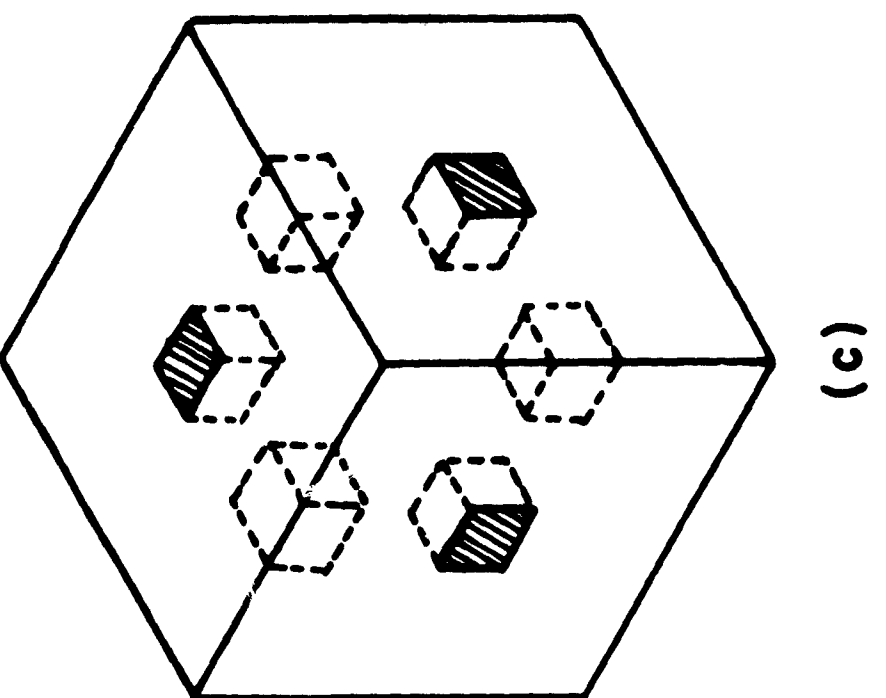
- 8. Combined plot of ductility of several copper dispersion alloys versus volume fraction.
- 9. True stress - strain curves plotted on logarithmic paper for a series of copper - chromium alloys containing various volume fractions of particles. Average particle diameter: 0.0016".
- 10. Strain hardening exponent,  $n$ , of several copper dispersion alloys plotted against volume fraction and reciprocal mean free path.
- 11. Combined plot of the strain hardening exponent of several copper dispersion alloys versus volume fraction
- 12. True fracture stress of several copper dispersion alloys plotted against volume fraction and reciprocal mean free path.
- 13. Combined plot of fracture stress of several copper dispersion alloys versus volume fraction.
- 14. Photomicrograph of the fracture region of a ductile copper-molybdenum alloy Volume fraction Mo-.058; Av. particle dia. 0.00019"; 600 X.
- 15. Photograph of copper strip specimens with drilled holes showing strain concentration lines between holes.
- 16. Combined plot of ductility versus volume fraction for copper specimens containing various second phases and for notched copper specimens.
- 17. The relation of yield stress to log reciprocal mean free path between particles in copper - chromium and copper - iron alloys (Gensamer plot).
- 18. Stages in preparation of copper powder compacts.
- 19. Standard tensile specimen
- 20. Typical microstructures of copper compact aggregates.
- 21. Typical microstructures of copper compact aggregates.



(a)

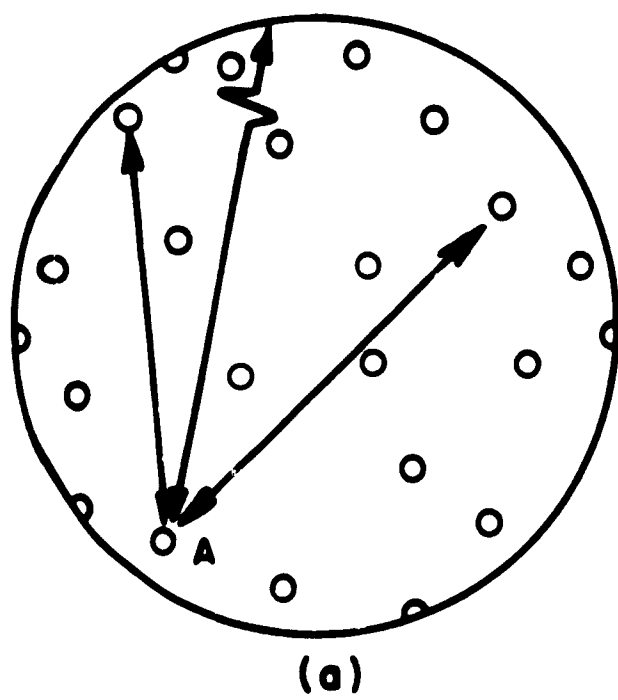


(b)

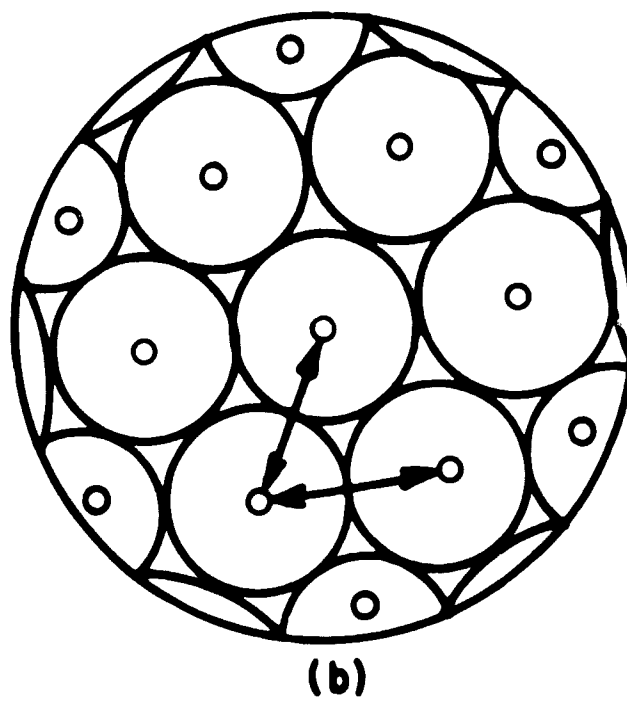


(c)

FIG. 1



MEAN FREE PATH,  $\lambda$



MEAN PARTICLE SPACING,  $D_s$

FIG. 2

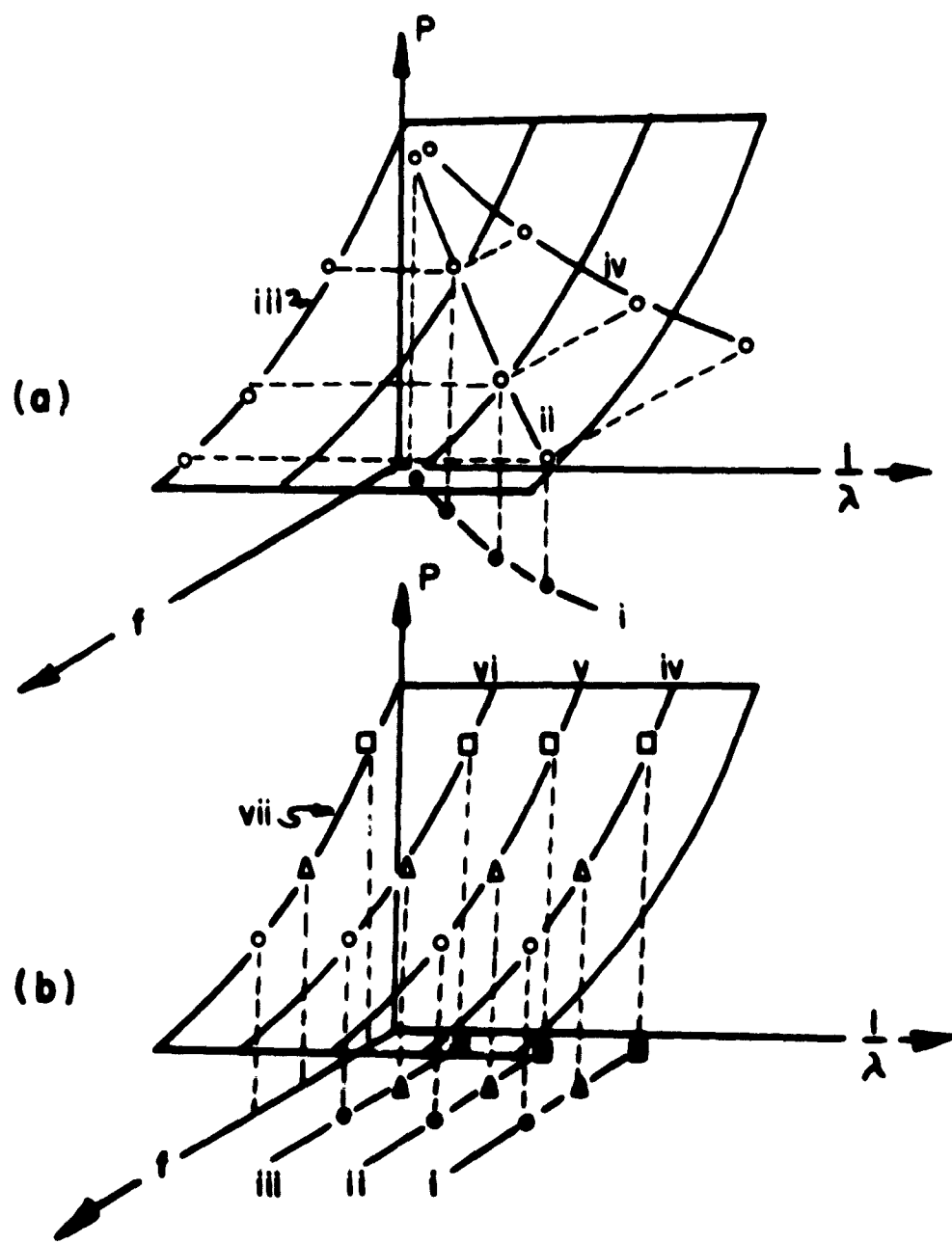


FIG. 3

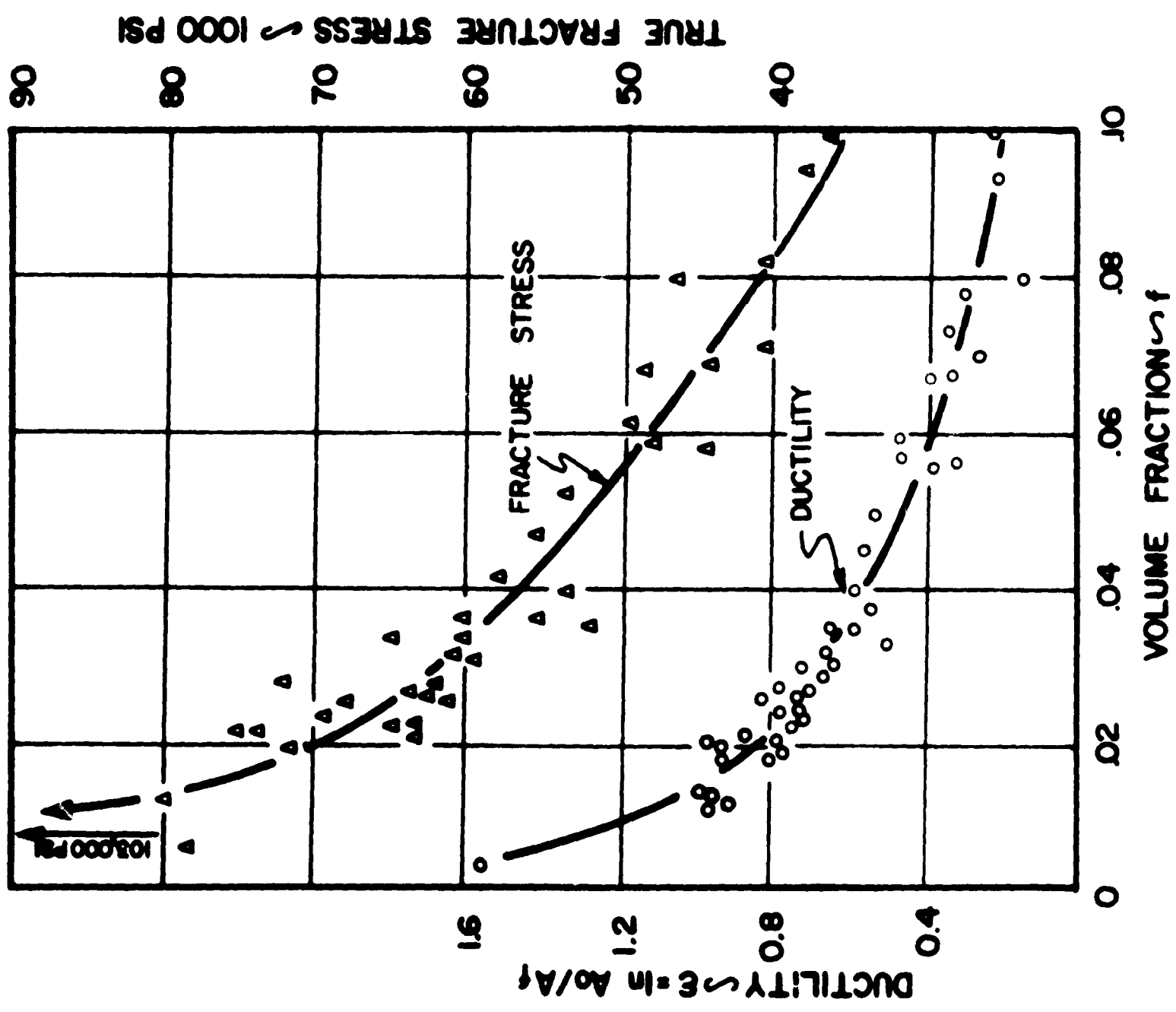
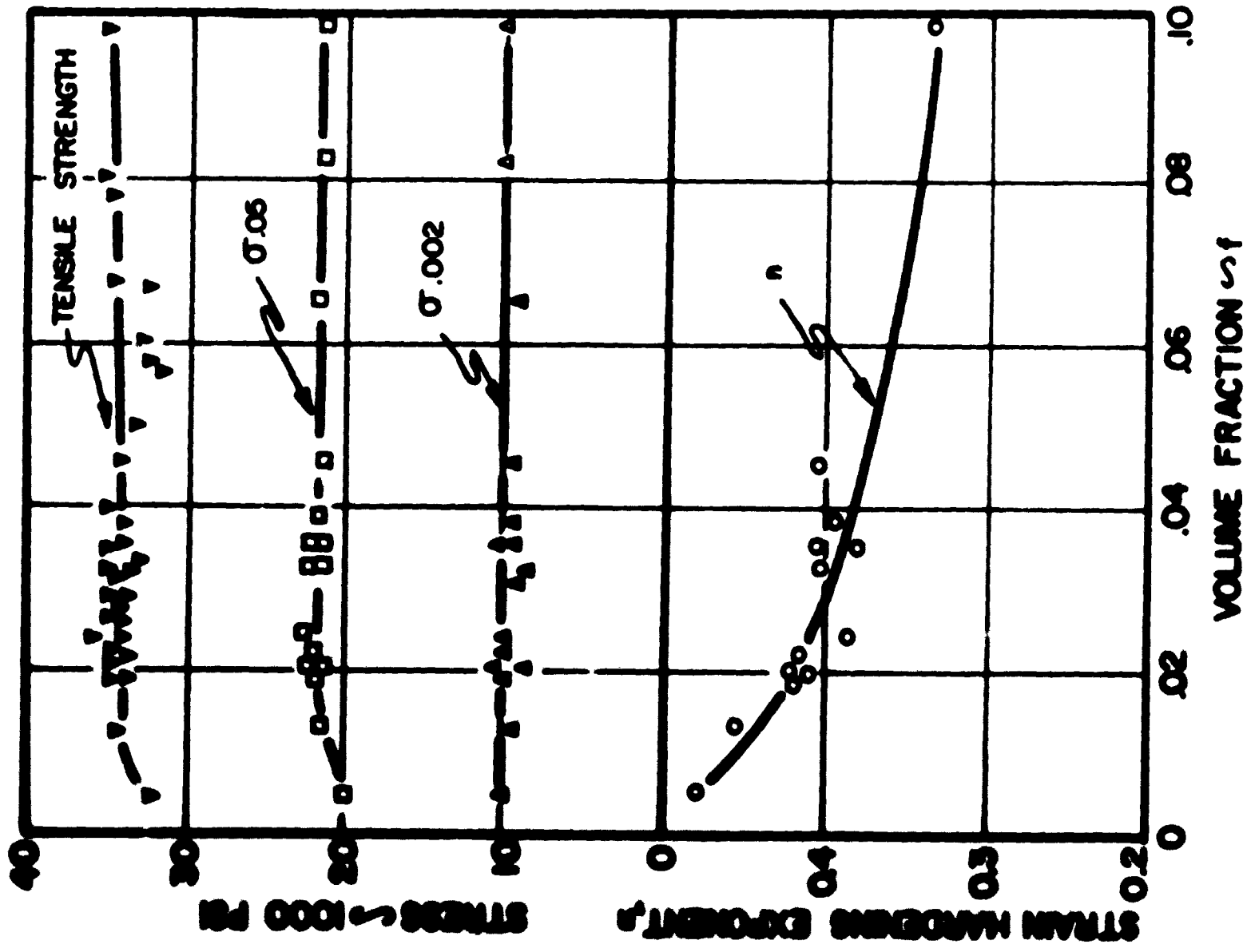


FIG. 4

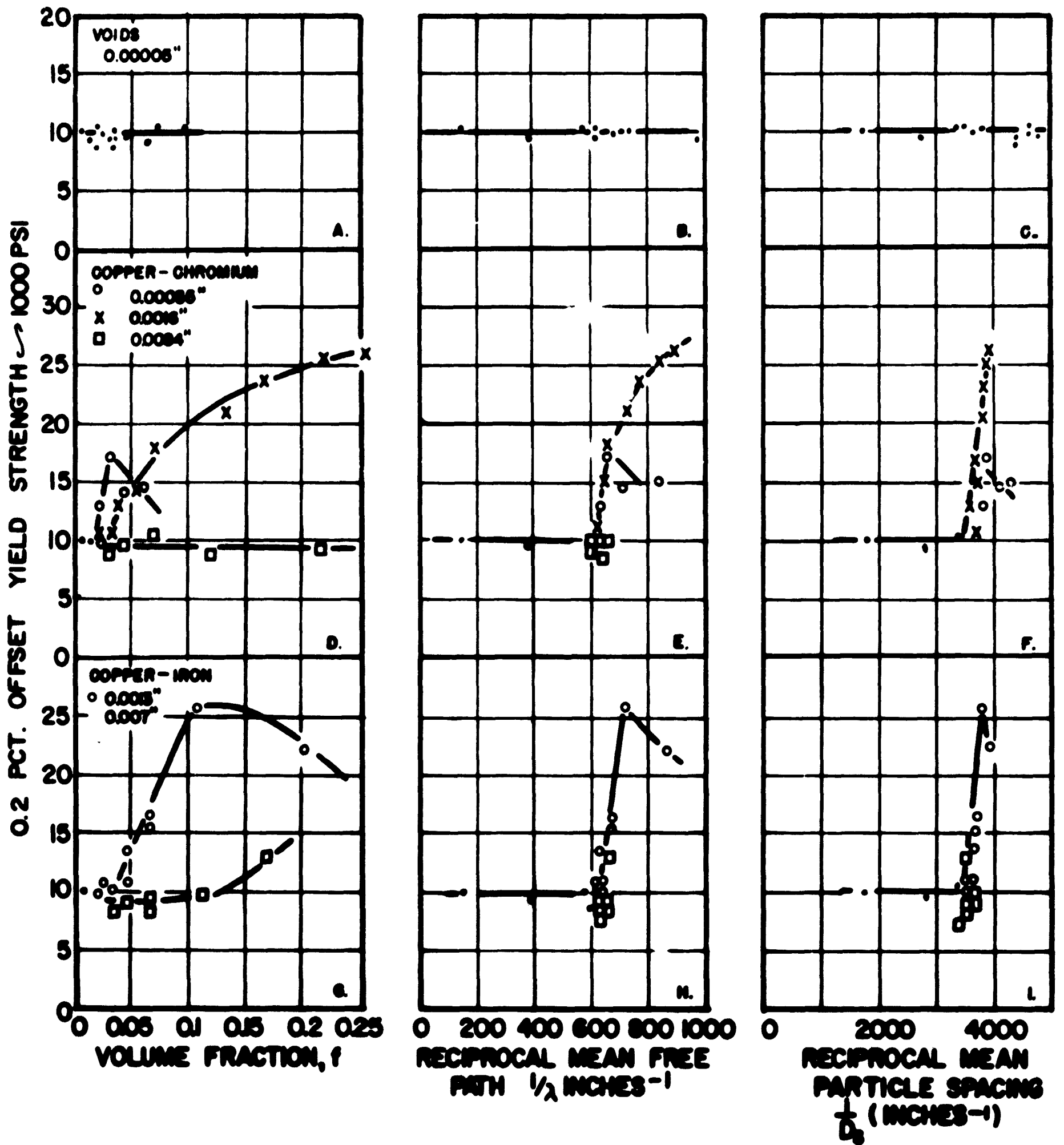


FIG. 5 (A TO I)

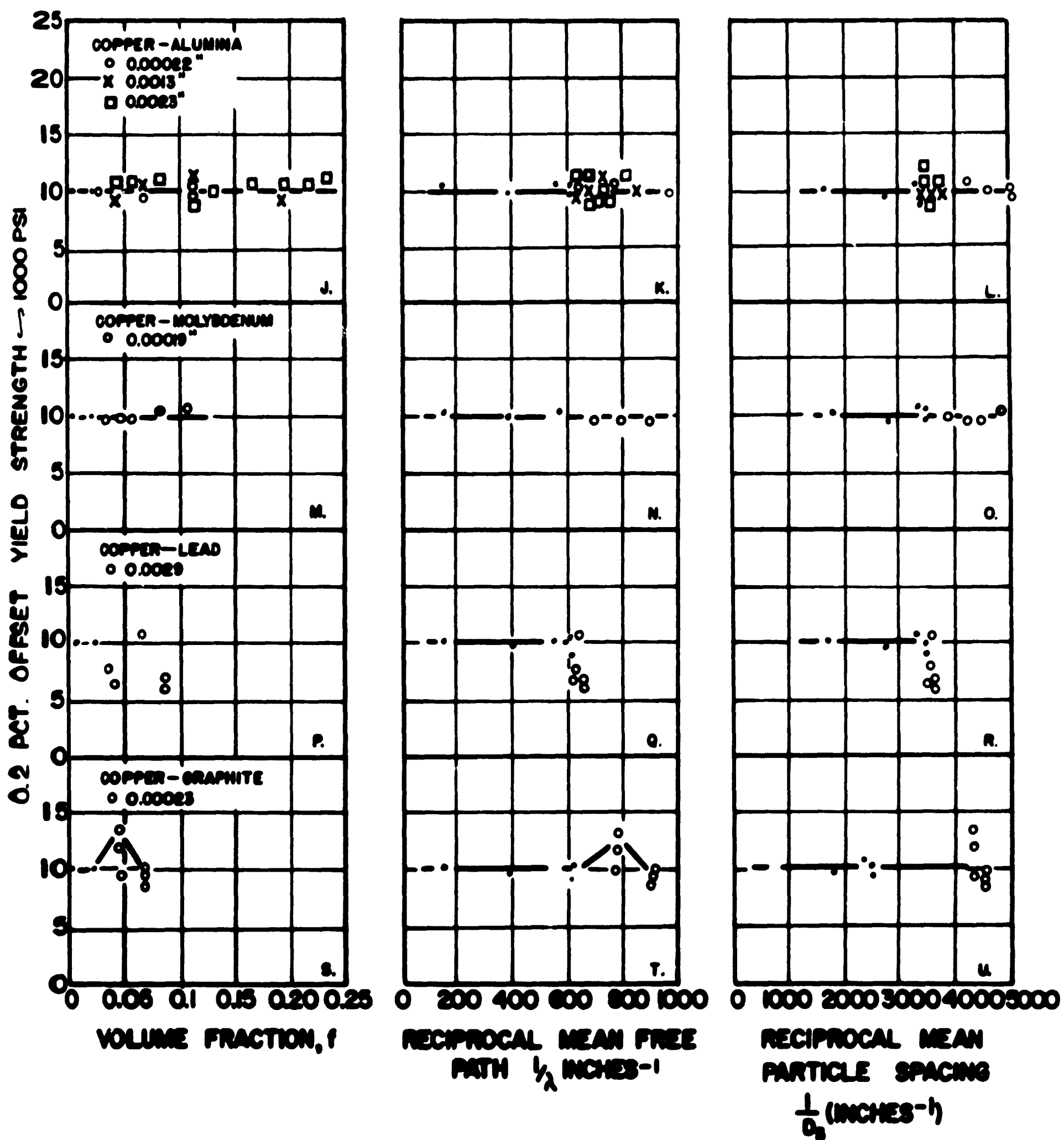
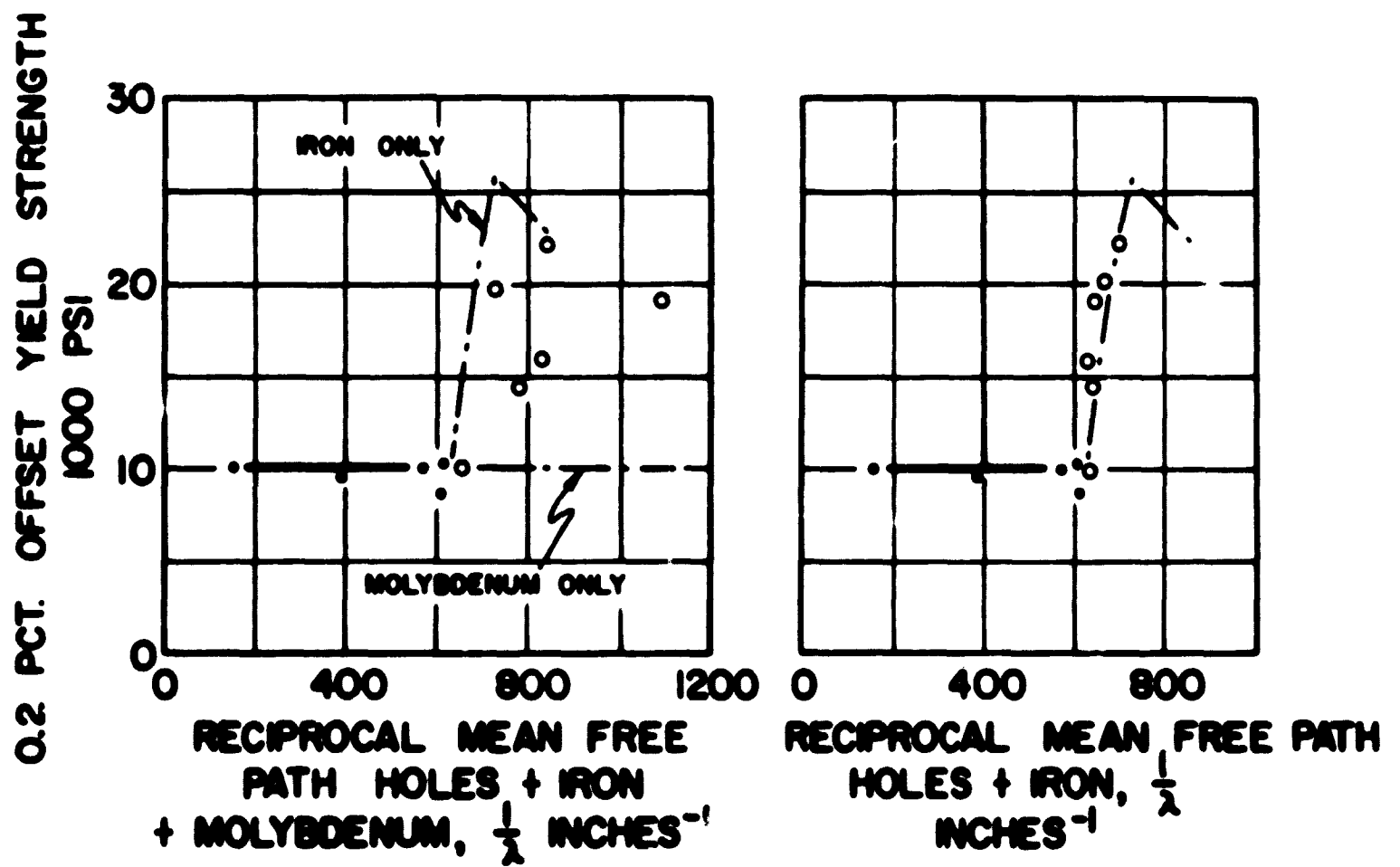


FIG. 5 (J TO U)





**FIG. 6**

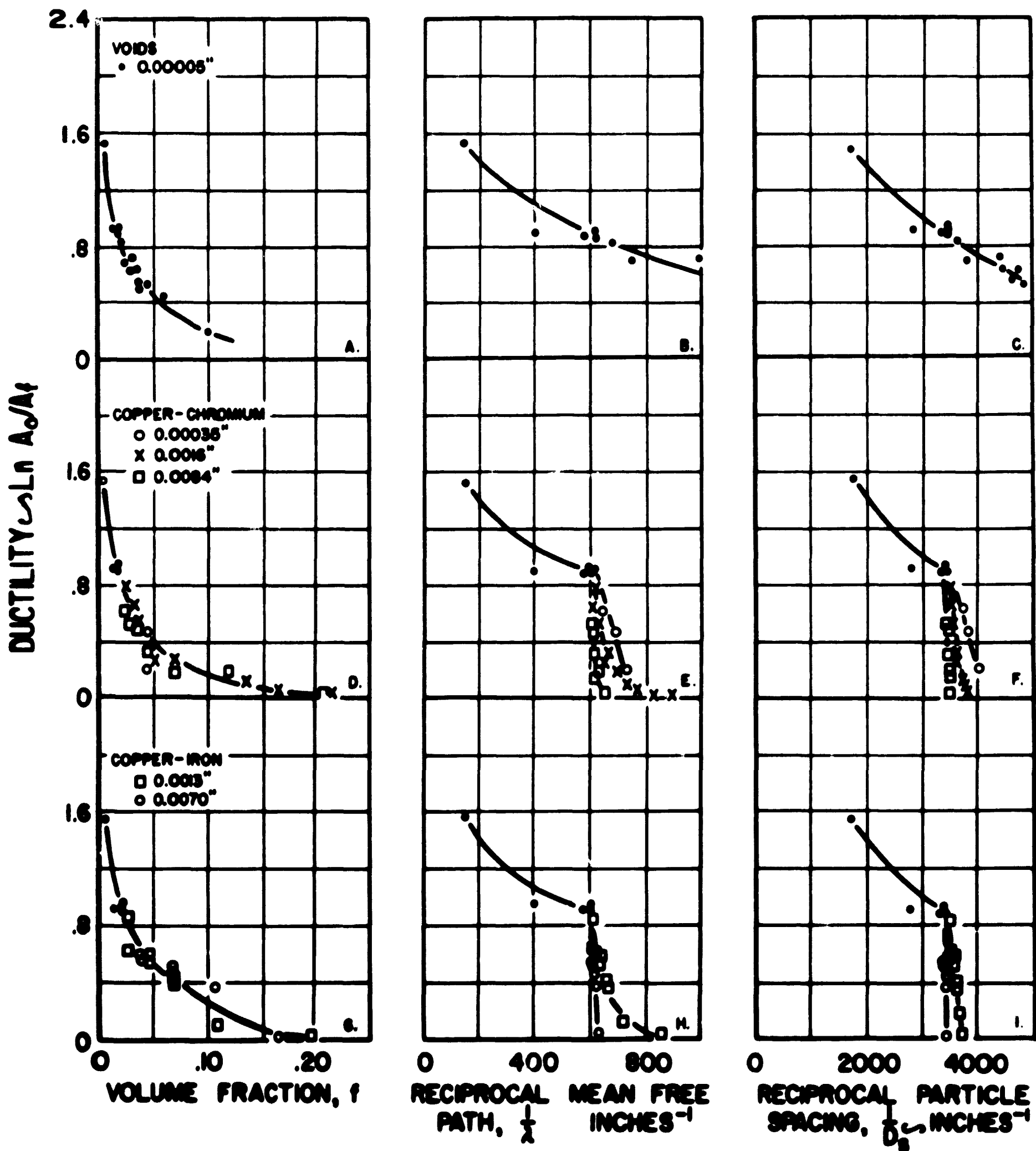


FIG. 7 (A TO I)

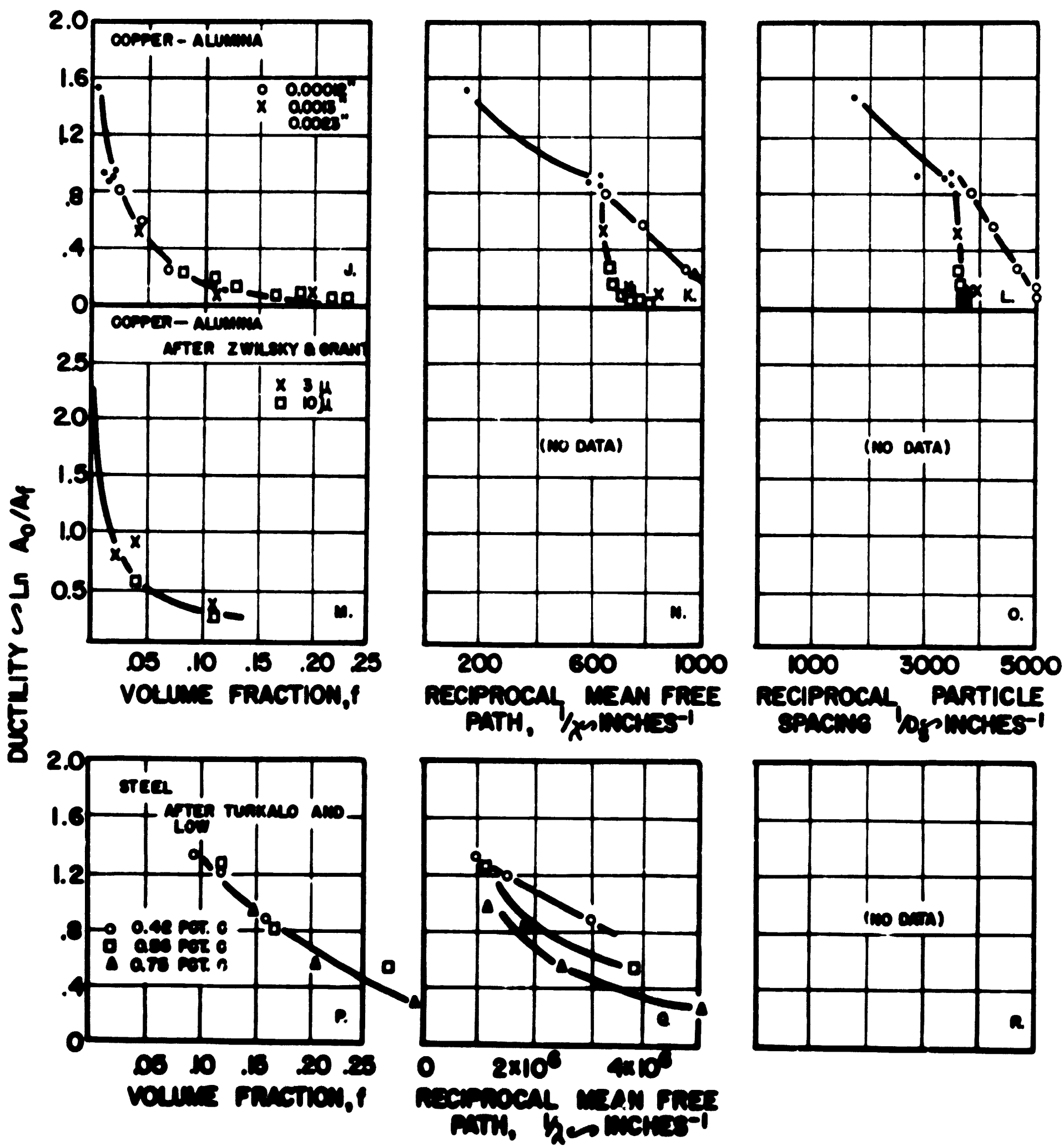


FIG. 7 (J TO R)



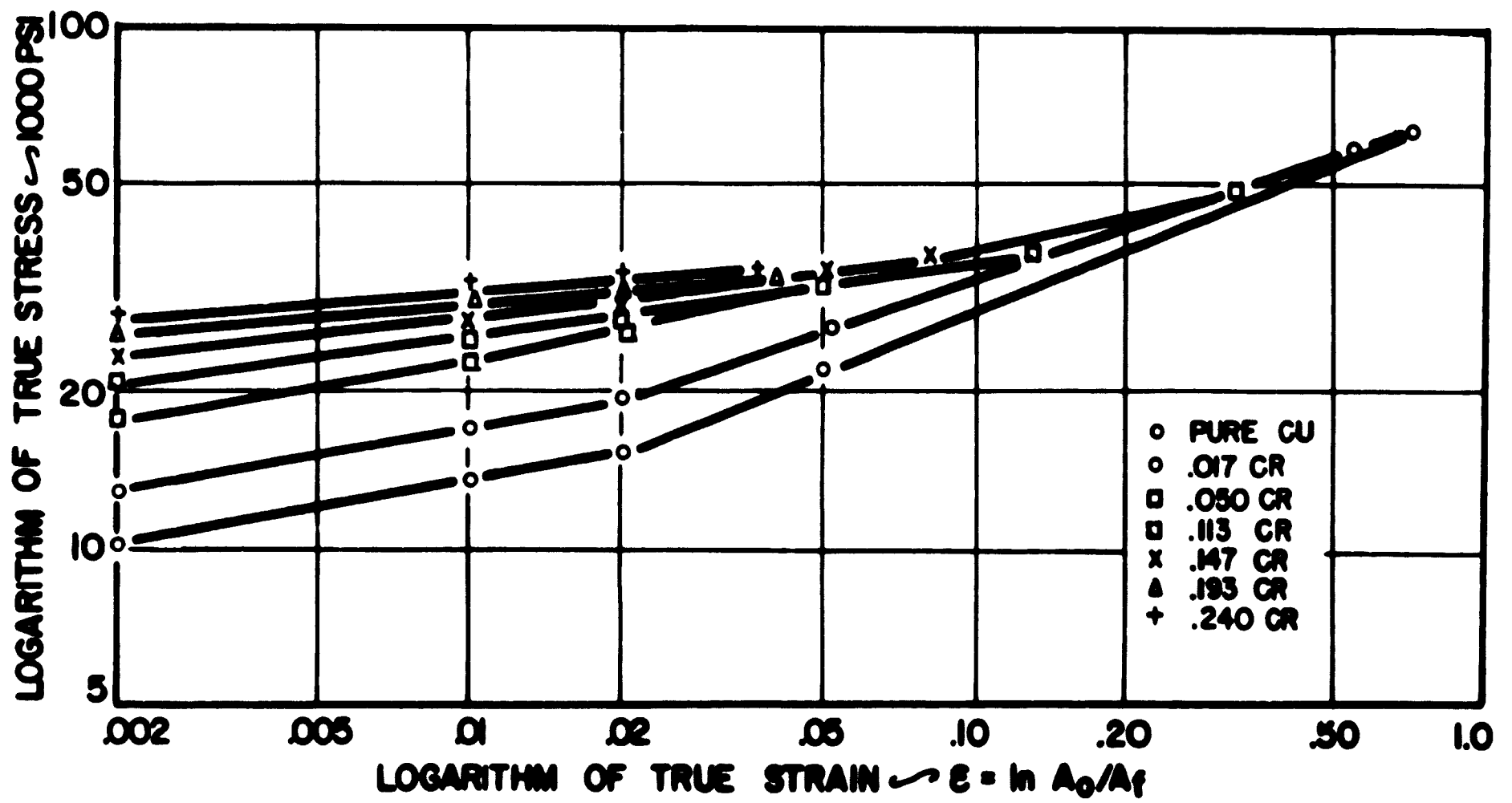


FIG. 9

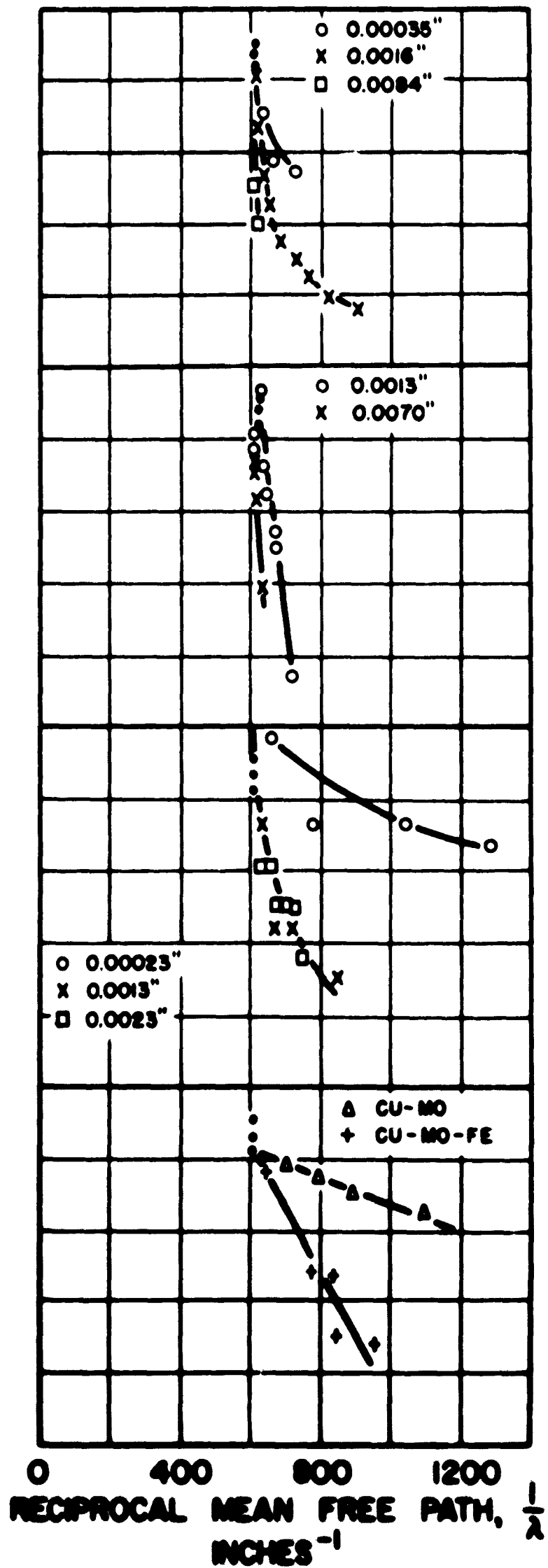
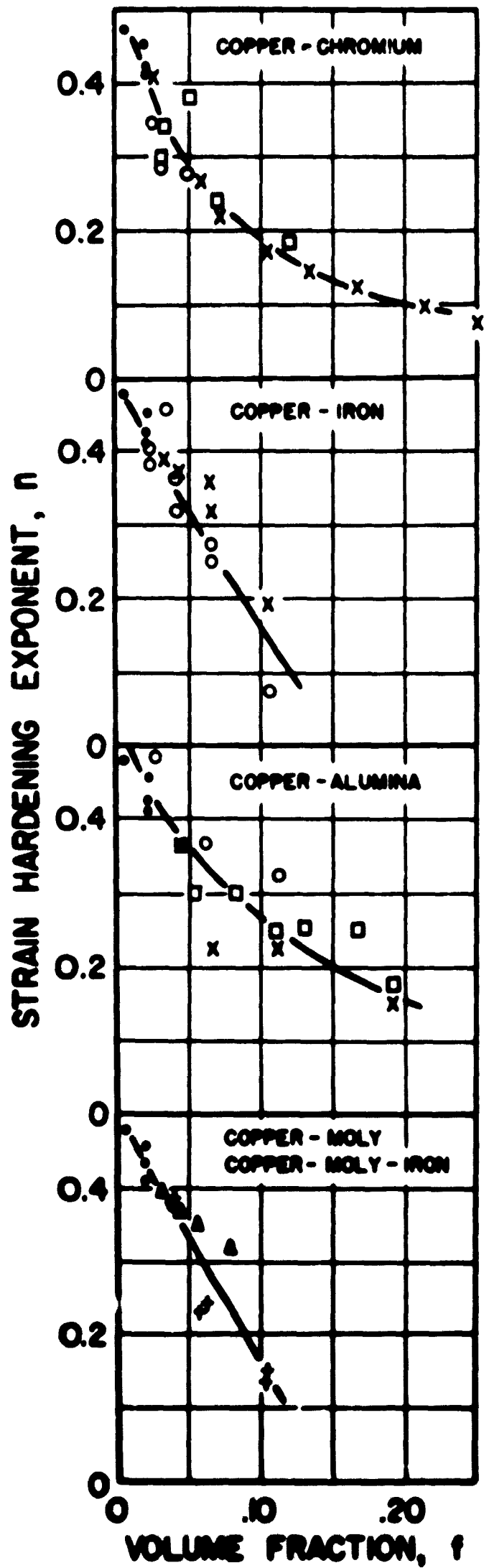


FIG. 10



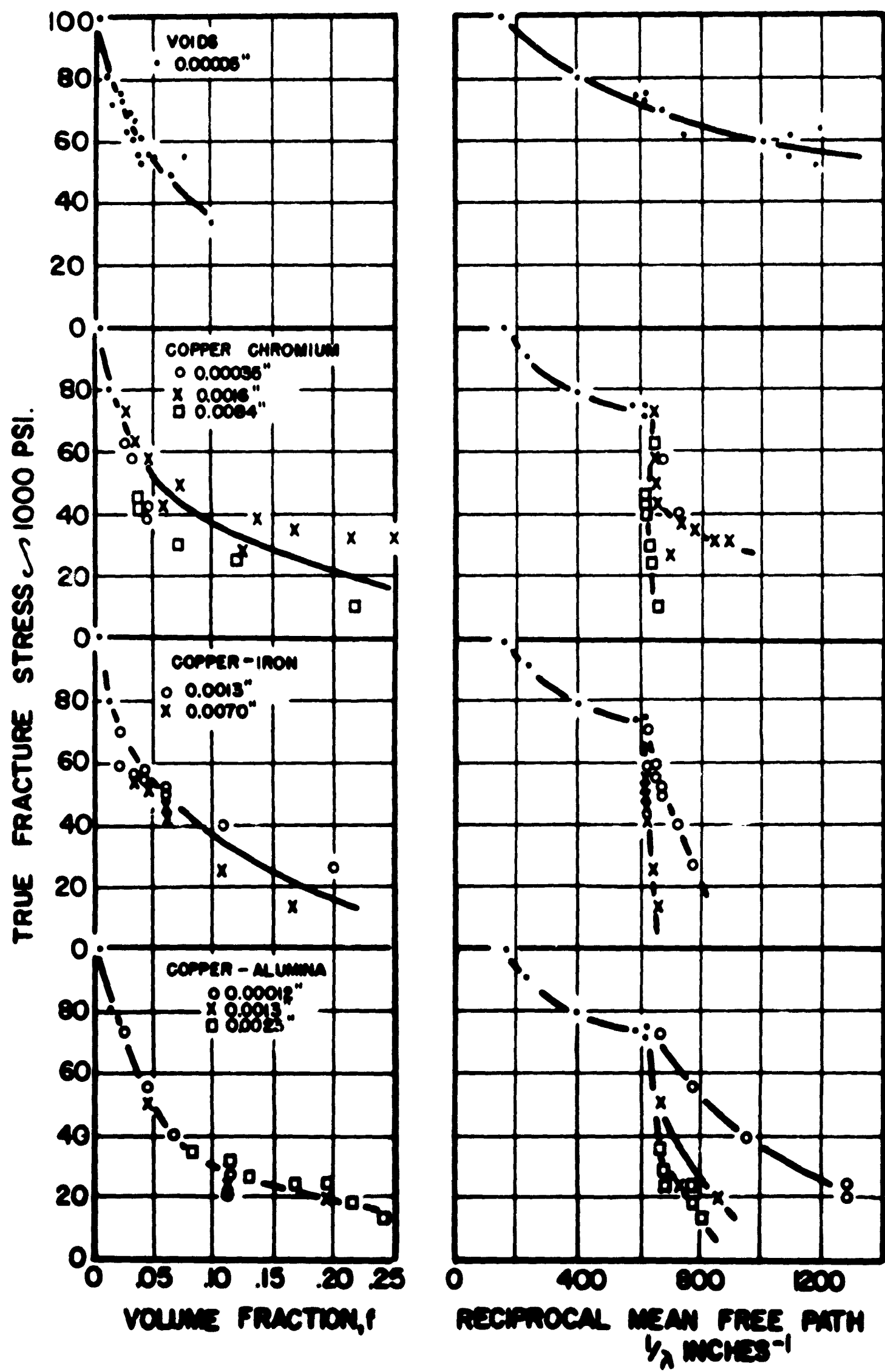


FIG. 12



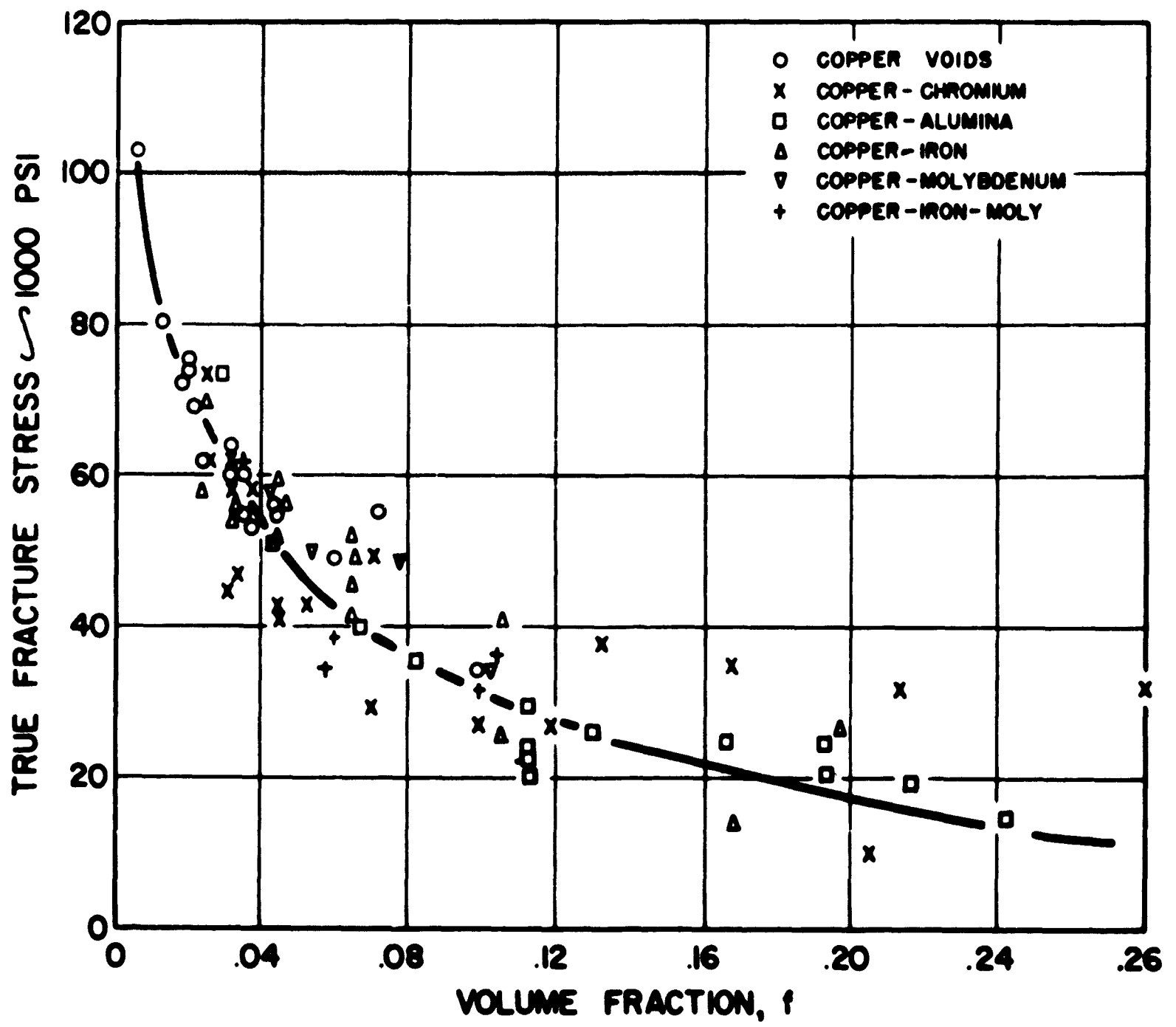
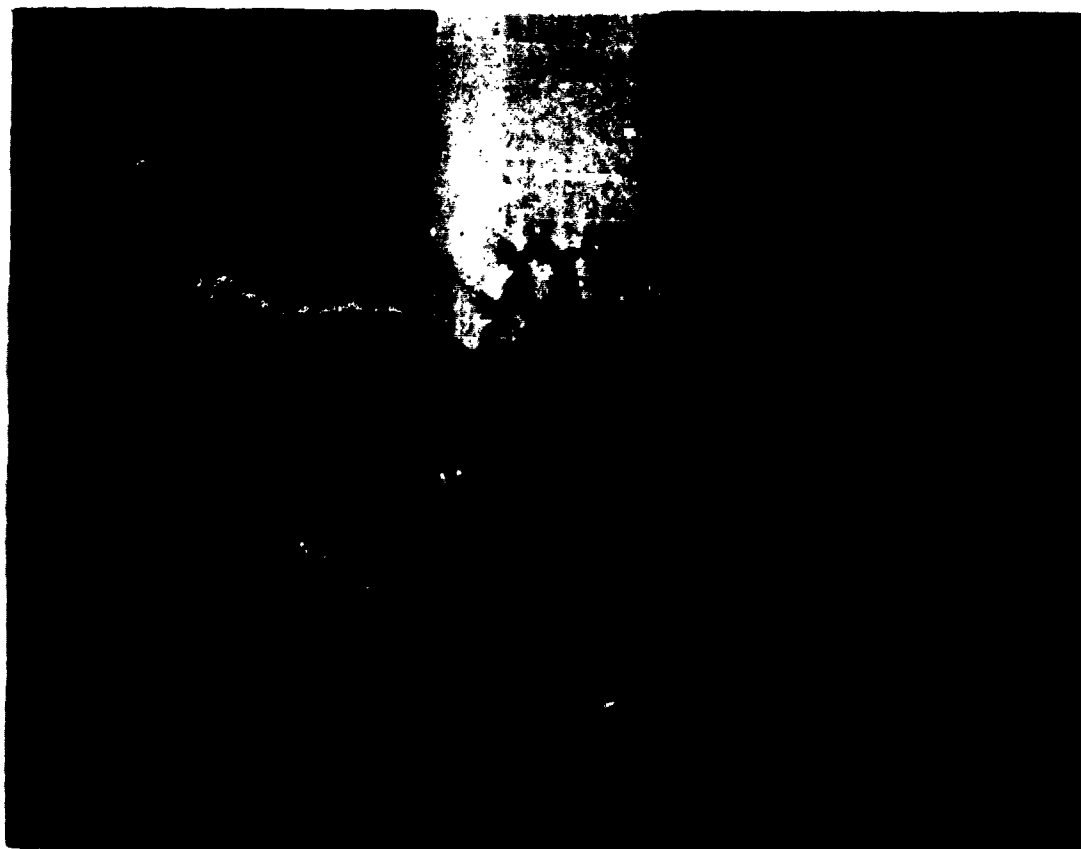


FIG. 13



**FIG.14 :PHOTOMICROGRAPH OF FRACTURE REGION  
OF DUCTILE COPPER-MOLYBDENUM ALLOY.  
VOLUME FRACTION Mo - 0.058; AVERAGE  
PARTICLE DIAMETER - 0.00019"; 600X.**



**FIG.15 :PHOTOGRAPH OF COPPER STRIP  
SPECIMEN WITH DRILLED HOLES  
SHOWING STRAIN CONCENTRATION  
LINES BETWEEN HOLES.**

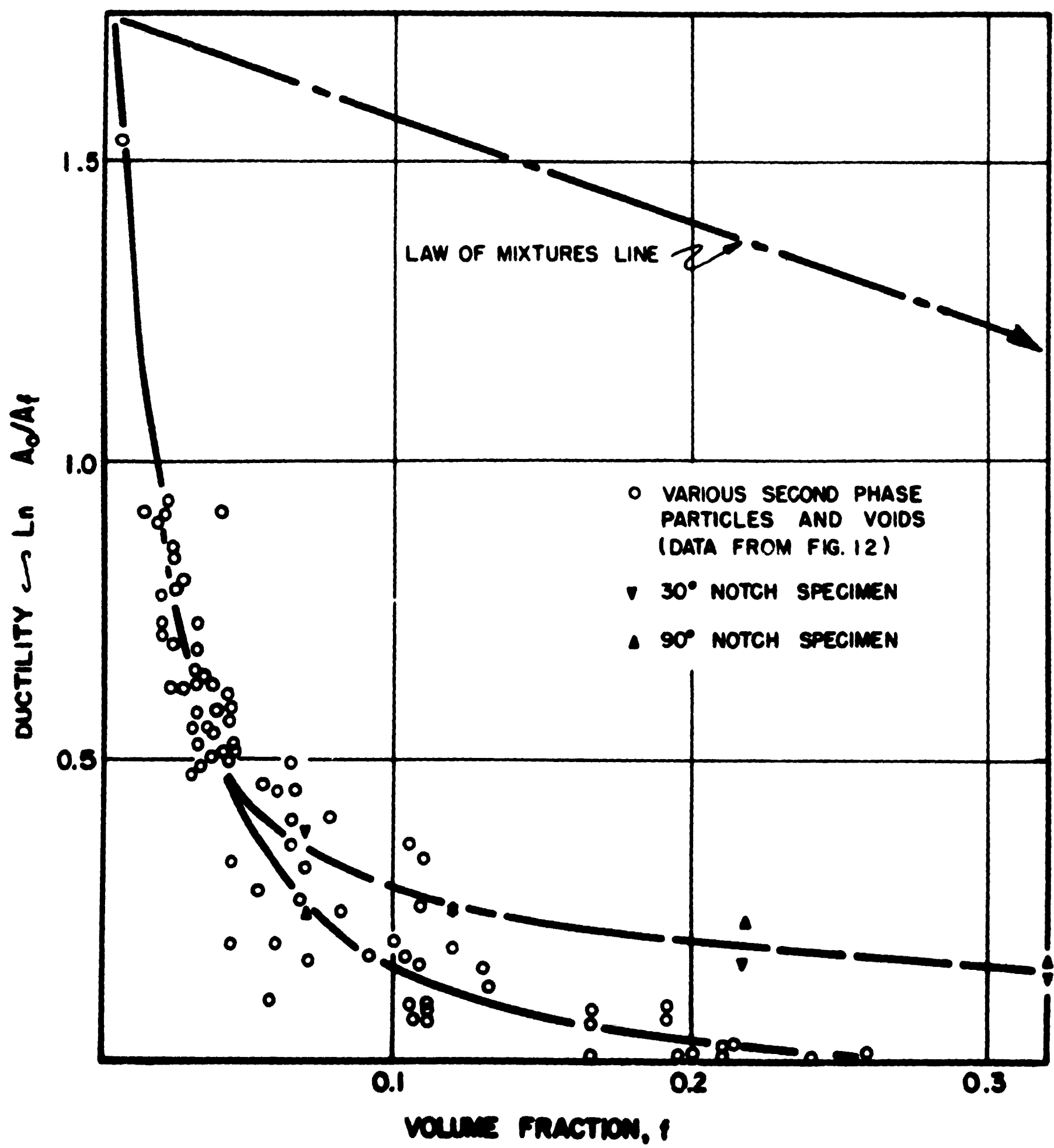


FIG. 16

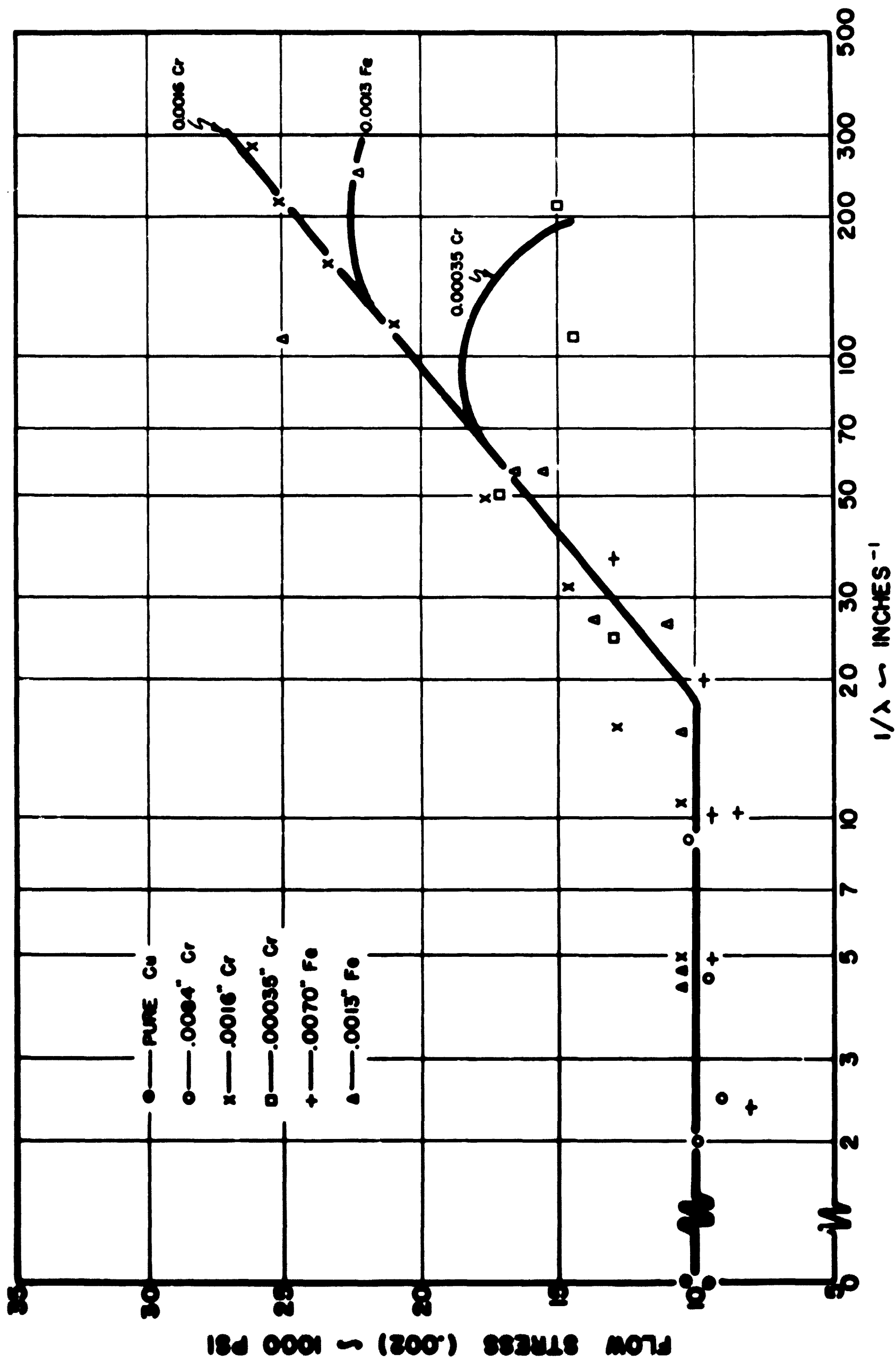
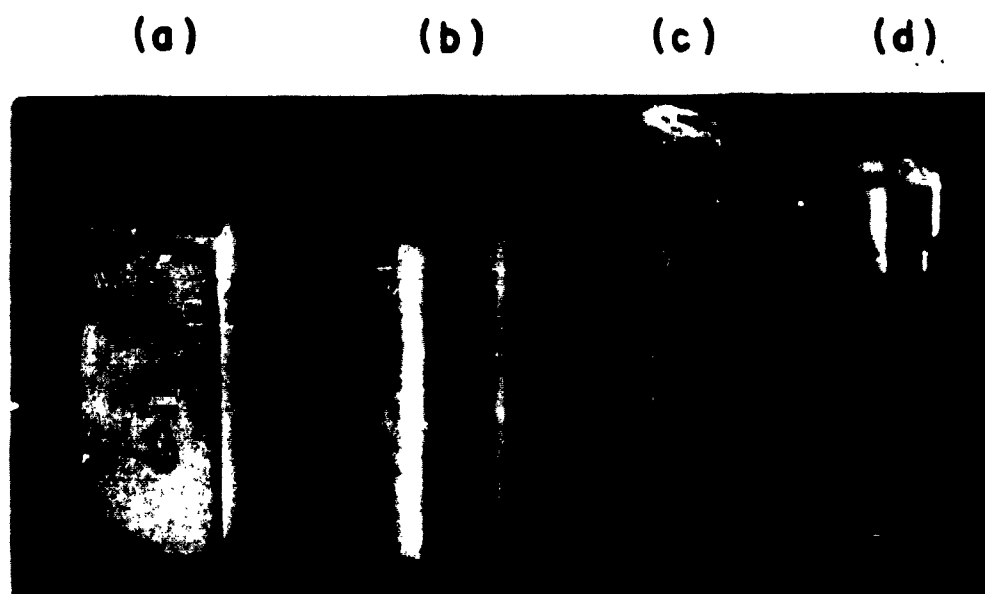
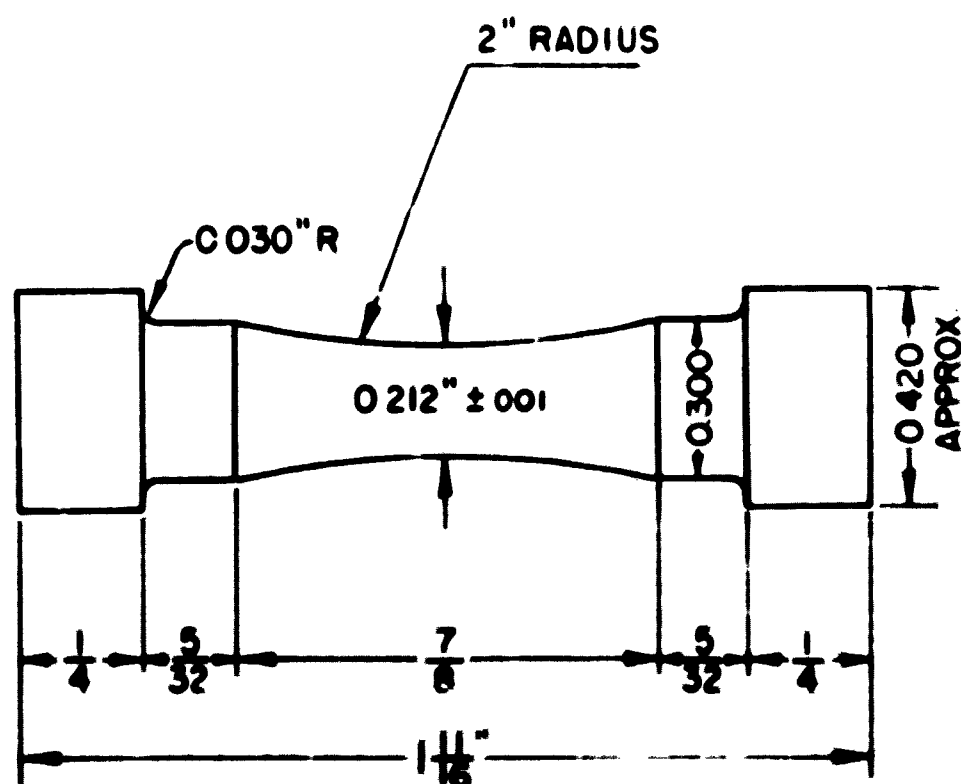


FIG. 17



**FIG. 18 : STAGES IN PREPARATION OF COPPER POWDER  
COMPACTS : (FROM LEFT TO RIGHT)**

- (a) SINTERED COMPACT 1.5" X .65" X .65"
- (b) .600" DIAMETER CYLINDER
- (c) SWAGED CYLINDER .420" DIAMETER (ONE END  
CUT OFF)
- (d) FINAL MACHINED SPECIMEN.



**FIG. 19: STANDARD TENSILE SPECIMEN.**



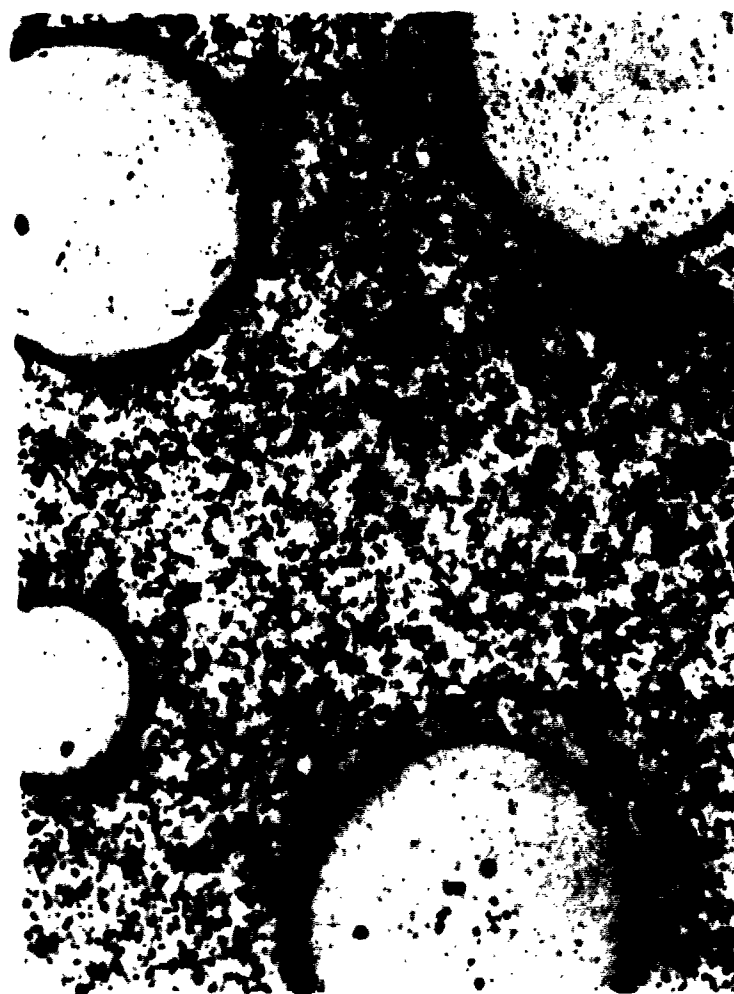
(a)



(b)



(c)



(d)

**FIG. 20: TYPICAL MICROSTRUCTURES OF Cu COMPACT AGGREGATES:**

(a) Cu + 4% HOLES, 600 X

(b) Cu + 6% Mn, .00019" AVERAGE DIAMETER, 600 X

(c) Cu + 10% Fe, .0013" AVERAGE DIAMETER, 100 X

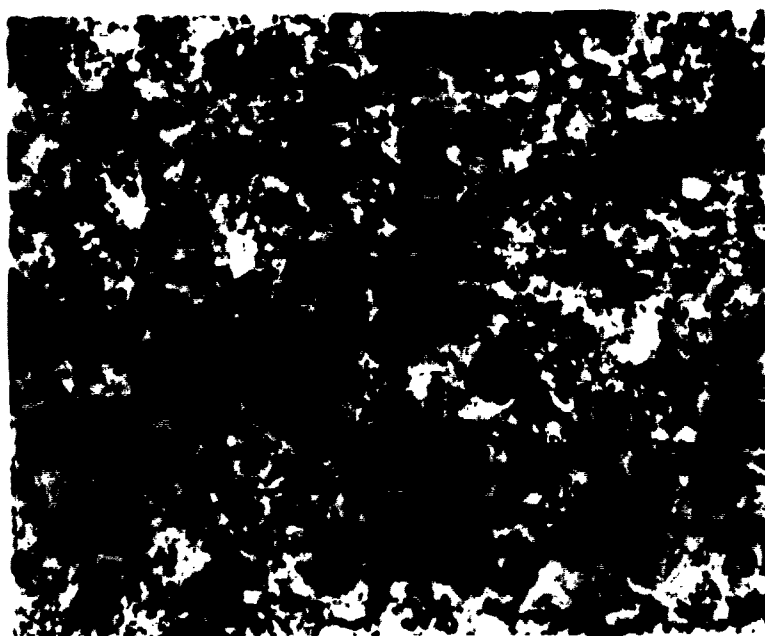
(d) Cu + 5% IRON BALLS, .023" AVERAGE DIAMETER, 75 X



(a)



(b)



(c)

**FIG.21: TYPICAL MICROSTRUCTURES OF COPPER COMPACTS:**

(a) COPPER + 10% CHROMIUM, AVERAGE DIA. .0016",  
75 X ;

(b) COPPER + 10% CHROMIUM, AVERAGE DIA. .0084",  
75 X ;

(c) COPPER + 10% ALUMINA, AVERAGE DIA. .0013",  
75 X .